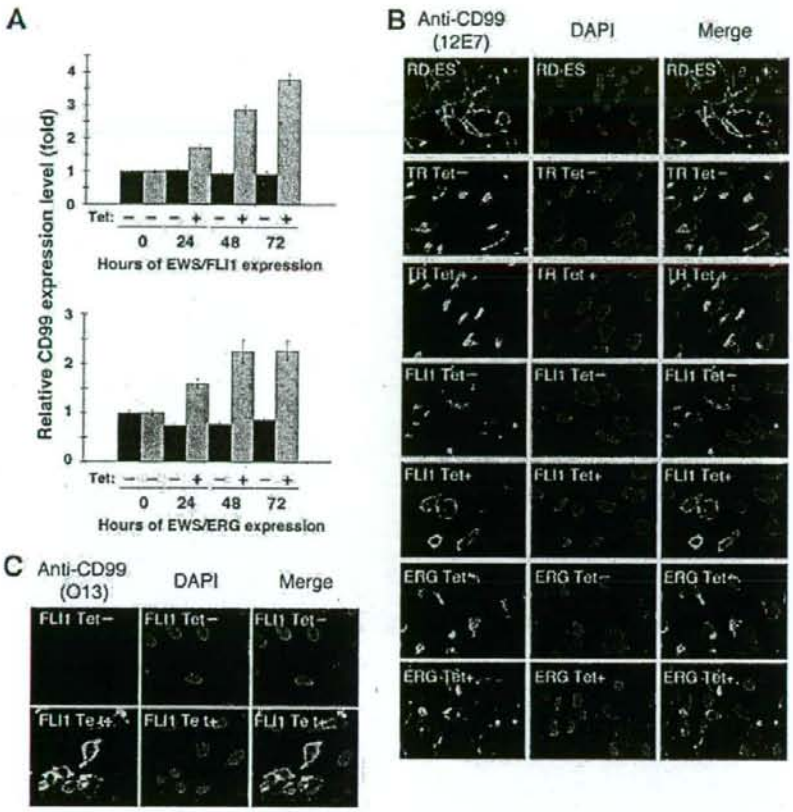

FIG. 3. Effects of tetracycline-mediated EWS/ETS expression on the expression and distribution of CD99 in UET-13 cells. (A) Relative CD99 levels in UET-13 transfectants in the absence or presence of tetracycline (Tet). UET-13 transfectants were treated with or without 3 μg/ml of tetracycline for the indicated periods. Real-time RT-PCR was performed to investigate the expression pattern of CD99. Signal intensities of CD99 were normalized using those of a control housekeeping gene (human GAPDH gene). Data are relative values with standard deviations from triplicate wells and are normalized to the mRNA level at 0 h, which is arbitrarily set to 1 in the graphical presentation. (B and C) Immunocytostaining of CD99 in UET-13 transfectants. Cells were cultured on coverslips in the absence or presence of tetracycline for 72 h and then stained with anti-CD99 antibody 12E7 (B) or O13 (C) as described in Materials and Methods. RD-ES cells were also examined as a positive control. For the staining of nuclei, DAPI was used.

Effect of EWS/ETS on CD99 expression in UET-13 cells. The p30/32MIC-2 gene product, CD99, is a cell surface glycoprotein expressed in EFT with a strong membranous staining pattern and thus constitutes a useful marker for EFT (2, 30). Knowing the dramatic change of morphology in UET-13 cells, we next investigated the mRNA level of CD99 in tetracycline-treated and untreated UET-13 transfectants by quantitative real-time RT-PCR. CD99 levels were clearly elevated by tetracycline treatment in both UET-13TR-EWS/FLI1 and UET-13TR-EWS/ERG cells in a time-dependent manner (Fig. 3A).

We also examined the protein expression of CD99 by immunostaining using 12E7 antibody, which is most widely used as an anti-CD99 antibody. An EFT cell line, RD-ES, showed strong membranous staining of CD99 (Fig. 3B), while neither UET-13TR cells nor UET-13 cells had such a staining. Of note is the fact that although 12E7 reactivity was observed only in the cytoplasm in perinuclear regions in both UET-13TR (Fig. 3B) and UET-13 (data not shown) cells, this antibody is well known to cross-react with a cytoplasmic protein not yet characterized. Since another anti-CD99 antibody, O13, did not react with either UET-13TR (Fig. 3C) or UET-13 (data not shown) cells, we concluded that the perinuclear staining of 12E7 mentioned above was a cross-reaction with unrelated proteins.

In the absence of tetracycline, both UET-13TR-EWS/FLI1 and UET-13TR-EWS/ERG cells were also negative with anti-CD99 antibodies (a pattern designated $CD99^-$), similar to UET-13 cells. Surprisingly, however, tetracycline induced a membranous staining pattern (designated $CD99^+$) in UET-13TR-EWS/FLI1 and UET-13TR-EWS/ERG cells, and some $CD99^+$ cells had irregularly contoured nuclei (Fig. 3B). The same results were observed with another anti-CD99 antibody, O13 (Fig. 3C), indicating that the membranous staining observed for UET-13 transfectants with the anti-CD99 antibodies

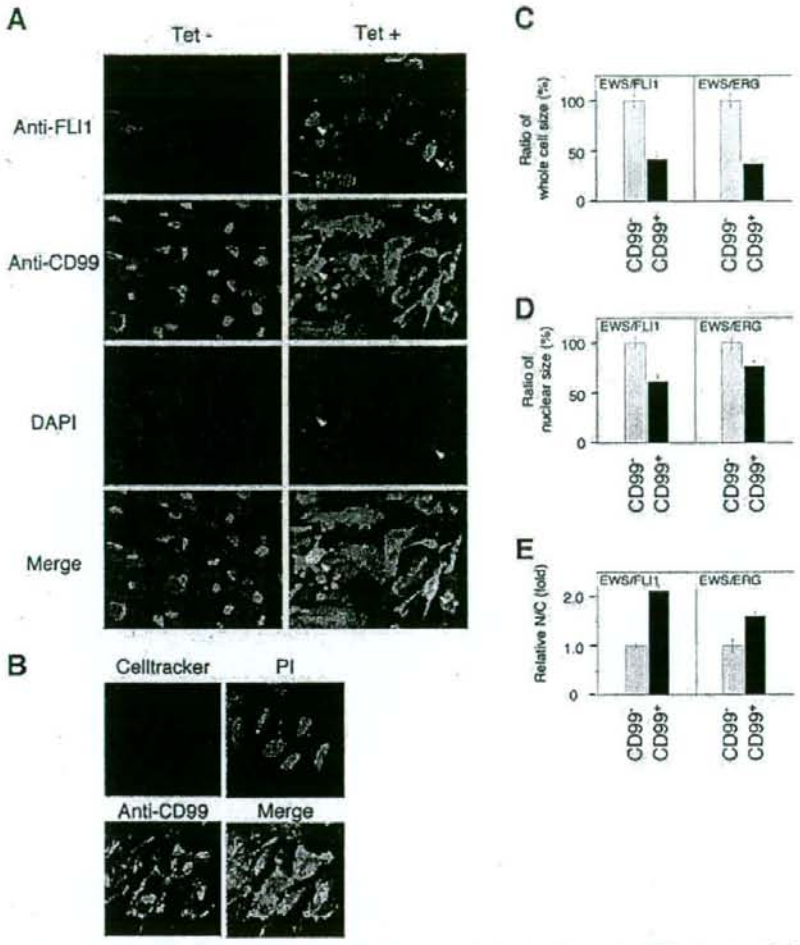

FIG. 4. EWS/ETS expression, alteration of CD99 distribution, and cell morphological changes in UET-13 cells. (A) Immunofluorescence studies using anti-Fli1 (red), anti-CD99 (green), and DAPI (blue). UET-13TR-EWS/FLI1 cells were cultured on coverslips in the absence or presence of tetracycline (Tet) for 72 h and then stained as described in Materials and Methods. White arrowheads indicate $CD99^+$ cells that have a strong staining pattern with anti-Fli1 antibodies and also have remarkable CD99 expression and morphological features. (B) Immunofluorescence analysis by triple staining with whole cells (Celltracker; blue), CD99 (anti-CD99; green), and nuclei (PI; red). UET-13TR-EWS/FLI1 cells were cultured as described for panel A and then stained as described in Materials and Methods. (C to E) Measurements of whole-cell size (C), nuclear size (D), and N/C ratio (E) in tetracycline-treated UET-13 transfectants. UET-13TR-EWS/FLI1 and UET-13TR-EWS/ERG cells were cultured on coverslips in the presence of tetracycline for 72 h and then stained as described in Materials and Methods. These samples were analyzed by the image analysis software Image J ($n = 50$). (C and D) Data are relative values with the SE and are normalized to the size of $CD99^-$ cells, which is arbitrarily set to 100. (E) Data are relative values with the SE and are normalized to the size of $CD99^-$ cells, which is arbitrarily set to 1.

was really CD99 derived. Despite the fact that cells were single colony derived, there was a heterogeneous response to tetracycline treatment in UET-13TR-EWS/FLI1 and UET-13TR-EWS/ERG cells, but most of the $CD99^+$ cells had a small round morphology, one of the characteristics of EFT. To assess the correlation between EWS/FLI1 expression and the change of the CD99 expression pattern, we performed immunofluorescence studies using anti-Fli1 and anti-CD99 antibodies. As shown in Fig. 4A, tetracycline treatment induced a marked enhancement of nuclear staining with anti-Fli1 antibodies in a large number of UET-13TR-EWS/FLI1 cells, indicating the induction of EWS/FLI1 proteins. Furthermore, we observed that the cells with a strong signal for Fli1 tended to reveal a membranous staining pattern with anti-CD99 antibodies and a small round morphology (Fig. 4A). To further verify the correlation between CD99 expression pattern and cell morphology, we estimated the size of cells by triple staining using Celltracker Blue, PI, and anti-CD99 antibody (Fig. 4B). As

TABLE 2. Immunophenotypic characterization of UET-13 transfectants and EFT cells

MPC status[a]	CD marker	Result for[b]: UET-13	UET-13TR		UET-13TR-EWS/FLI1		UET-13TR-EWS/ERG		RD-ES	EFT status[c]	SK-ES1
		Tet$^-$	Tet$^+$	Tet$^-$	Tet$^+$	Tet$^-$	Tet$^+$				
M+	CD29	+	+	+	+	+	+	+	+	+	
M+	CD59	+	+	+	+	+	+	+	+	+	
M+	CD90	+	+	+	+	+	+	+	+	+	E+
M+	CD105	+	+	+	+	+	+	+	+	+	
M+	CD166	+	+	+	+	+	+	+	+	+	
M+	CD44	+	+	+	+	+	+	+	−	−	
M+	CD73	+	+	+	+	+	+	+	−	−	
M+	**CD10**	+	+	+	+	**Down**	+	**Down**	−	−	
M+	**CD13**	+	+	+	+	**Down**	+	**Down**	−	−	
M+	**CD49e**	+	+	+	+	**Down**	+	**Down**	+	−	
M+	**CD61**	+	+	+	+	**Down**	+	**Down**	−	−	
M+	**CD55**	+	+	+	+	**Down**	+	+	+	−	
M+	**CD54**	−	−	−	−	**Up**	−	**Up**	+	+	E+
M(−)	**CD117**	−	−	−	−	**Up**	−	**Up**	+	+	E+
M+/−	**CD271**	−	−	−	−	**Up**	−	**Up**	+	+	E+
	CD40	−	−	−	−	−	−	−	+	+	E+
	CD56	−	−	−	−	−	−	−	+	+	E+
M(−)	CD133	−	−	−	−	−	−	−	+	+	
M(−)	CD14	−	−	−	−	−	−	−	−	−	
M(−)	CD34	−	−	−	−	−	−	−	−	−	
M(−)	CD45	−	−	−	−	−	−	−	−	−	

[a] M(−), negative for MPCs; M+/−, positive for BM-derived MPCs but negative after in vitro culture; M+, positive for MPCs.
[b] +, most cells positive; −, negative; Up, up-regulated by tetracycline treatment; Down, down-regulated by tetracycline treatment. Boldface indicates the antigens the immunophenotypes of which were changed in favor of EFT. Tet$^-$, tetracycline negative; Tet$^+$, tetracycline positive.
[c] E+, positive for EFTs.

presented in Fig. 4C and D, the results clearly showed that the majority of CD99$^+$ cells were significantly smaller in both whole-cell size and nuclear size than the CD99$^-$ cells. Moreover, CD99$^+$ cells also had a substantially increased N/C ratio (Fig. 4E). These results indicated that EWS/ETS expression promoted CD99 expression in UET-13 cells, and CD99 expression status is correlated with the degree of morphological change.

EWS/ETS expression altered the immunophenotype of UET-13 cells. Human MPCs reveal a characteristic expression of several surface antigens and can be identified on the basis of the reactivity with a set of monoclonal antibodies against CD antigens (25, 42). On the other hand, some CD antigens are characteristically expressed on EFT cells (17, 28, 33). Using the combinations of these antibodies listed in Table 2, which are useful for the immunodetection of either MPCs or EFT cells, we further examined whether EWS/ETS expression affects the immunophenotype of UET-13 cells and compared its effect with that on the immunophenotype of EFT cell lines (Table 2 and Fig. 5). As shown in Table 2, UET-13 cells express most of the human primary MPCs markers. Some of the antigens expressed in MPCs, namely, CD29, CD59, CD90, CD105, and CD166, were also found to be expressed in EFT cell lines, but others, namely, CD10, CD13, CD44, CD61, and CD73, were not. In contrast, antigens recognized to be present in EFT cells, including CD40, CD56, and CD133, were absent from UET-13 cells. Interestingly, when the effect of tetracycline-mediated EWS/ETS expression on the immunophenotype of UET-13 cells was tested, levels of some of the antigens present in UET-13 cells, such as CD10, CD13, and CD61, were found to be decreased (Fig. 5). In contrast, some of the markers found in EFT cells, i.e., CD54, CD117, and CD271, became positive in UET-13TR-EWS/ETS cells after tetracycline treatment. Because UET-13TR cells did not show such immunophenotypic change upon treatment with tetracycline, these results indicated that, at least in part, the immunophenotype of UET-13 cells was changed in favor of EFT in the presence of EWS/ETS.

EWS/ETS in UET-13 cells modulates EFT-like gene expression. To further examine the molecular mechanism of EWS/ETS-dependent cellular modulation in human mesenchymal progenitor background, we performed DNA microarray-based expression profiling using the Affymetrix human genome U133 Plus 2.0 array. As a first step to this approach, we validated our experimental systems by analyzing the sequential changes of known EWS/ETS target genes, i.e., inhibitor of differentiation 2 (ID2) (14, 39), NK2 transcription factor related, locus 2 (NKX2.2) (9, 48), and insulin-like growth factor binding protein 3 (IGFBP3) (41). Consistent with previous reports, levels of ID2 and NKX2.2 increased with the expression of EWS/ETS in a time-dependent manner, whereas the expression level of IGFBP3 decreased (Fig. 6A). Employing the same procedure, we also examined whether the change of surface antigen expression was regulated at the transcriptional level and determined the mRNA expression levels of some surface antigens in UET-13 transfectants with or without tetracycline treatment. In accordance with the results of immunocytometric and immunohistological experiments, the mRNA expression levels of CD10, CD13, CD49e, and CD61 were decreased, while those of CD54, CD99, CD117, and CD271 were markedly increased in tetracycline-treated UET-13TR-EWS/ETS cells (Fig. 6B and C), indicating that the expression of these antigens is

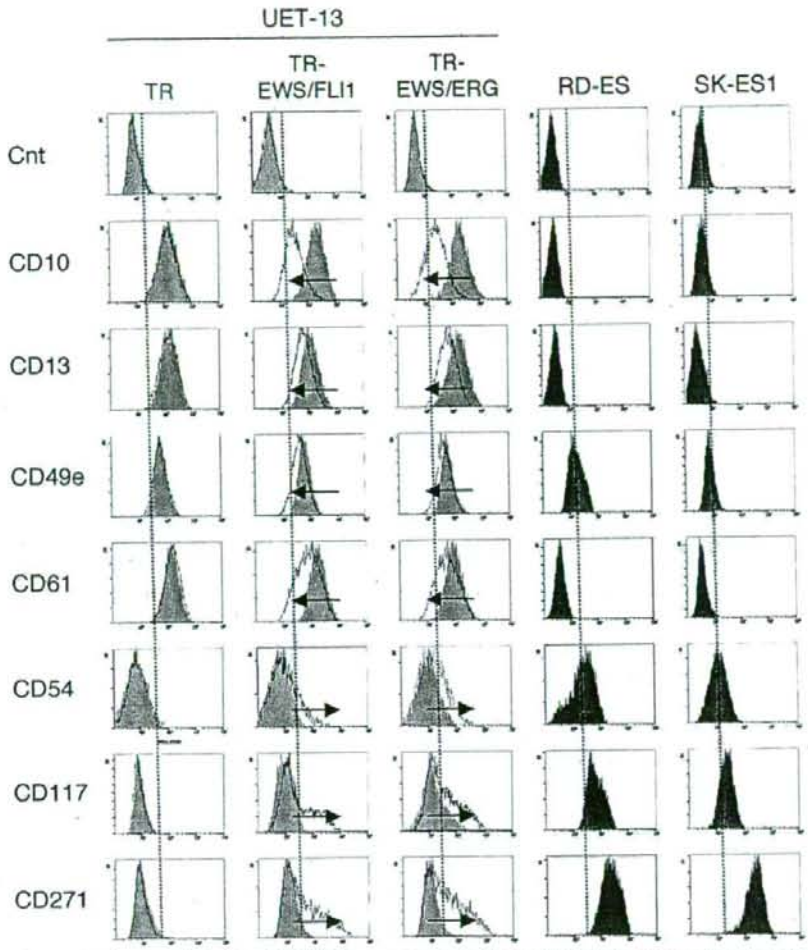

FIG. 5. Immunophenotypic change on induction of EWS/ETS expression in UET-13 cells. UET-13 transfectants were cultured with or without 3 μg/ml of tetracycline for 1 week and flow cytometric analyses were performed by using a set of antibodies as indicated. The histograms of UET-13 transfectants with (empty) and without (gray) tetracycline treatment were overlaid. Dotted lines indicate fluorescence intensities in negative control panels (Cnt). Arrows indicate the immunophenotypic change caused by tetracycline. The immunophenotypes of the EFT cell lines RD-ES and SK-ES1 were also examined.

controlled at the transcriptional level in the presence of EWS/ETS.

We next investigated the candidate genes whose expression is regulated by EWS/ETS in human MPCs. First, we selected the genes with up-regulated or down-regulated expression by EWS/ETS induction using gene cluster analysis (Fig. 7A; UET-13TR-EWS/FLI1 up, 4,294 probes; down, 4,103 probes; UET-13TR-EWS/ERG up, 3,358 probes; down, 3,705 probes). To reduce the number of the candidate genes, we selected up-regulated genes that are expressed in tetracycline-treated cells at least 1.5-fold higher than in untreated cells (UET-13TR-EWS/FLI1, 1,137 probes; UET-13TR-EWS/ERG, 835 probes). Similarly, the down-regulated genes that are expressed in tetracycline-treated cells at least 0.75-fold lower than in untreated cells (UET-13TR-EWS/FLI1, 1,803 probes; UET-13TR-EWS/ERG, 773 probes). By selecting common probes in both cells, we finally identified a group of candidate genes significantly controlled by EWS/ETS induction in the human mesenchymal progenitor background. Since microarray analysis was performed as a global screening in a single experiment, it is likely that there is a fair bit of noise in the derived gene profiles due to the lack of replicate data. This may account in part for the limited overlap between the profiles induced by EWS-FLI1 and EWS-ERG, whereas we still identified 349 probes of common up-regulated genes and 293 probes of common down-regulated genes (see the supplemental material). In addition to the EFT-specific genes mentioned above, these contained those previously described as EFT-specific genes, such as those for OB-cadherin/cadherin-11 (31), Janus

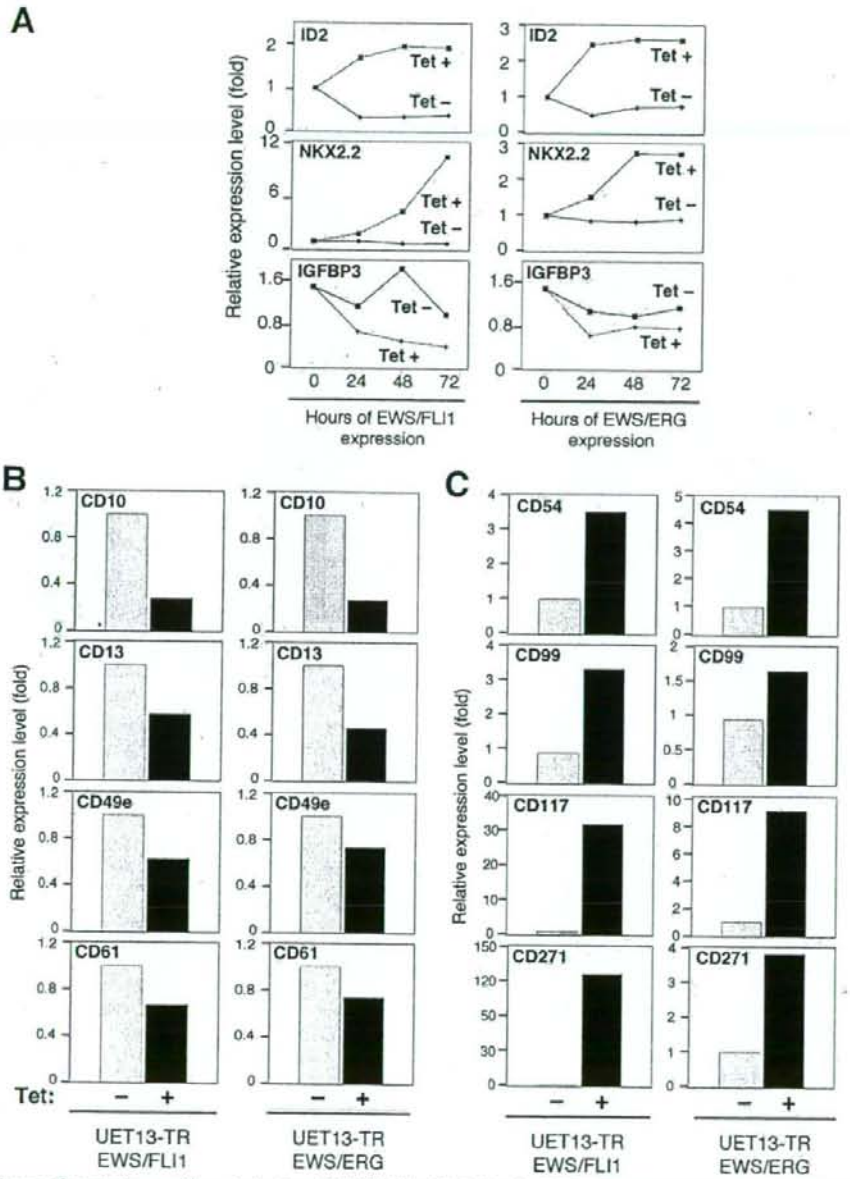

FIG. 6. The change of expression profile on induction of EWS/ETS in UET-13 cells. UET-13TR-EWS/FLI1 and UET-13TR-EWS/ERG cells were cultured in the absence or presence of tetracycline (Tet) for the indicated periods and analyzed using the Affymetrix human genome U133 Plus 2.0 array as described in Materials and Methods. (A) The sequential changes of ID2, NKX2.2, and IGFBP3 mRNA levels in UET-13 transfectants upon treatment with or without tetracycline. Diamond symbols indicate UET-13 transfectants in the absence of tetracycline; box symbols indicate UET-13 transfectants in the presence of tetracycline. (B and C) Microarray studies for the determination of expression profiles of surface antigens in UET-13 transfectants. UET-13 transfectants were treated with or without 3 μg/ml of tetracycline for 72 h. mRNA levels were determined with the Affymetrix human genome U133 Plus 2.0 array.

kinase 1 (JAK1) (49), keratin 18, and six-transmembrane epithelial antigen of the prostate (STEAP) (22). The expression pattern of these genes (642 probes) in UET-13 transfectants in the absence or presence of tetracycline is shown in the gene cluster in Fig. 7B. The expression of these genes was indeed changed significantly after EWS/ETS expression in both cells. They included genes associated with signal transduction (such as those for epidermal growth factor receptor, FAS [CD95], and fibroblast

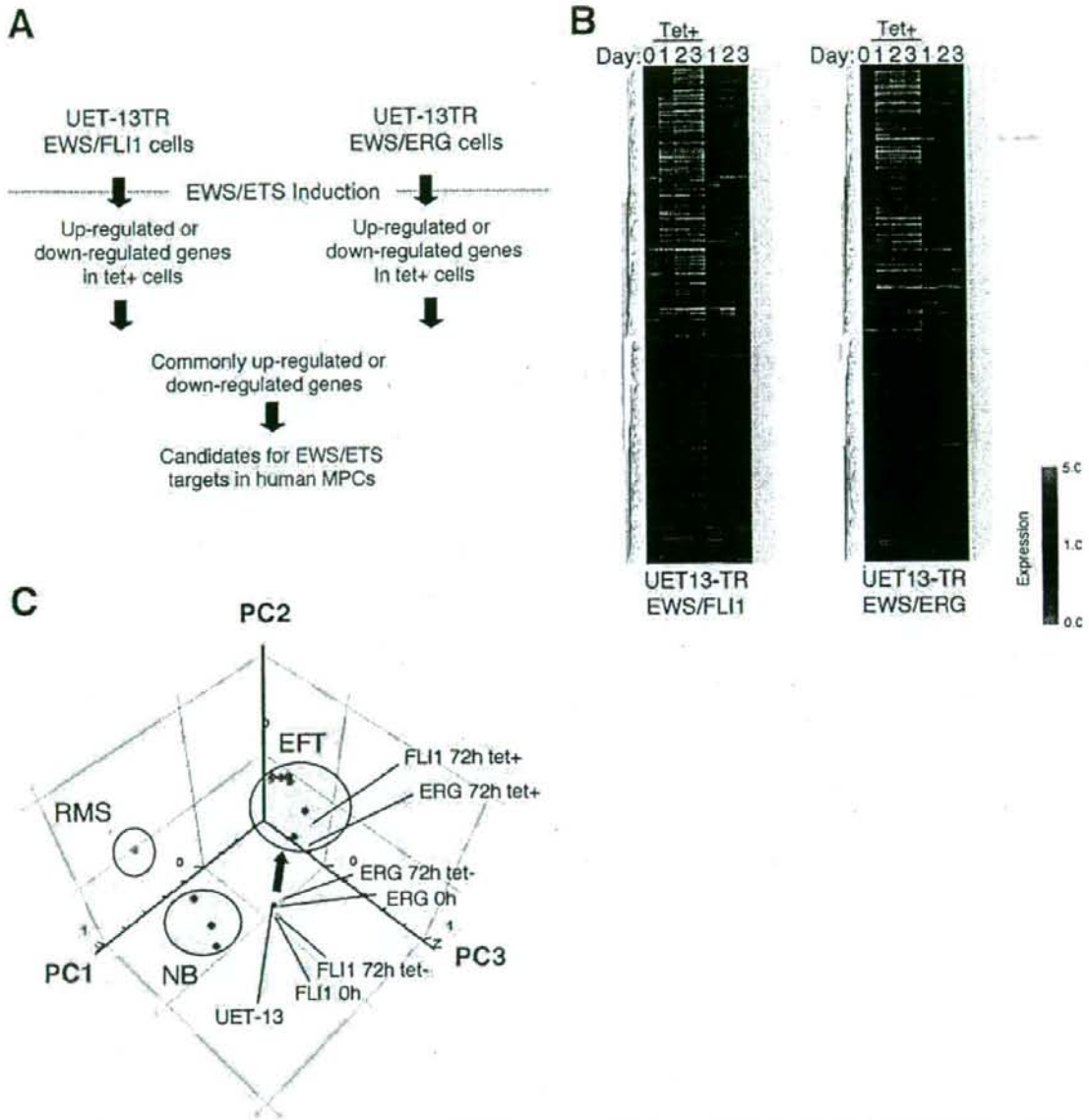

FIG. 7. Identification of candidates for the target of EWS/ETS in human MPCs by use of a microarray. UET-13TR-EWS/FLI1 and UET-13TR-EWS/ERG cells were cultured as described for Fig. 6 and analyzed using the Affymetrix human genome U133 Plus 2.0 array as described in Materials and Methods. (A) Scheme for the analysis of microarray data. (B) Gene cluster analysis of UET-13 transfectants in the absence or presence of tetracycline by use of 642 candidate genes for targets of EWS/ETS in human MPCs. (C) Visualization of sequential change by the gene expression profile in UET-13 transfectants following tetracycline-mediated EWS/ETS expression based on a PCA of 642 candidate genes. Deep blue plots indicate UET-13 cells. Light blue plots indicate UET-13 transfectants in the absence of tetracycline for 72 h. Yellow plots indicate UET-13 transfectants in the presence of tetracycline for 72 h. The pink circle indicates EFT cell lines expressing EWS/FLI1 (purple plots), EWS/ERG (red plot), and EWS/E1AF (light green plot). The light blue circle with blue plots indicates NB cell lines. The yellow circle with an orange plot indicates a rhabdomyosarcoma (RMS) cell line. Cutoff induction and repression levels are 1.5-fold and 0.75-fold, respectively. Tet, tetracycline.

growth factor receptor 1) and development (such as jagged-1 and frizzled-4, -7, and -8). Interestingly, in addition to the surface antigens presented in Fig. 6B and C, the expression profiling of EWS/ETS-expressing UET-13 cells displayed the modulation of several genes associated with cell adhesion, cytoskeletal structure, and membrane trafficking, such as those for collagen-11 and -21, ephrin receptor-A2, -B2, and -B3, ephrin-B1, claudin-1, integrin-α11, -αM, and -β2, CD66 (carcinoembryonic antigen-related cell adhesion molecule-1), and CD102 (intercellular cell adhesion molecule-2). They also included genes of chemokines CCL-2 and -3. These data raise the possibility that EWS/ETS can contribute to the membrane condition in human MPCs via the regulation of these cell surface molecules and chemokines.

Using these genes, we performed a PCA to visualize the shift in the gene expression pattern among the 642 probes. As shown in Fig. 7C, the plots of UET-13 transfectants treated with tetracycline became closer to those of EFT cells than to those of UET-13 transfectants without tetracycline treatment. These results indicated that the expression pattern of these genes was altered from that of UET-13 cells to that of EFT cells in an EWS/ETS-dependent manner. Since the gene expression profile of UET-13 cells is similar to those of other cell types of mesenchymal origin (data not shown), our results highlighted that the phenotypic alteration from mesenchyme to EFT-like cells in UET-13 cells induced by tetracycline treatment was accompanied by a change in the global gene expression profile.

EWS/ETS expression enhances the Matrigel invasion of UET-13 cells. To assess the role of EWS/ETS in malignant transformation in human MPCs, UET-13 transfectants were examined by invasion assay. As shown in Fig. 8A, tetracycline treatment did not affect the Matrigel invasion ability of UET-13TR cells. When examined similarly, however, tetracycline treatment resulted in an apparently increased invasion ($P < 0.05$) for both UET-13TR-EWS/FLI1 (Fig. 8B) and UET-13TR-EWS/ERG (Fig. 8C) cells. The results indicated that EWS/ETS expression can induce Matrigel invasion properties in human MPCs.

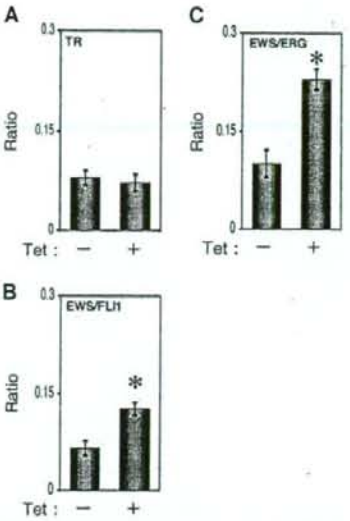

FIG. 8. Effects of EWS/ETS expression on the Matrigel invasion ability of UET-13 cells. UET-13TR (A), UET-13TR-EWS/FLI1 (B), and UET-13TR-EWS/ERG (C) cells were cultured in the absence or presence of tetracycline (Tet) for 72 h and then plated (2.5×10^4) on Matrigel-coated or uncoated filter inserts. After 20 h of culture, invading cells were stained with hematoxylin-eosin and counted in five fields per membrane as described in Materials and Methods. *, $P < 0.05$.

DISCUSSION

In the present study, using UET-13 cells as a model of human MPCs, we demonstrated that ectopic expression of EWS/ETS promoted the acquisition of an EFT-like phenotype, including cellular morphology, immunophenotype, and gene expression profile. Moreover, EWS/ETS expression enhances the ability of UET-13 cells to invade Matrigel. This assay is thought to mimic the early steps of tumor invasion in vivo (34), and the ability to penetrate the Matrigel has been positively correlated with invasion potential in several studies. Therefore, we concluded that EWS/ETS expression could mediate a part of the feature of tumor transformation in human MPCs. Thus, our culture system would provide a good model for testing the effects of EWS/ETS in human MPCs.

Several lines of evidence have indicated the transforming ability of EWS/FLI1, whereas that of EWS/ERG is not yet to be clarified. Therefore, it is noteworthy that our data demonstrated that EWS/ERG could promote an EFT-like phenotype in UET-13 cells similarly to EWS/FLI1. Thus, EWS/ERG also has the ability to induce an EFT-like phenotype in the human system. The major steps in the development of EFT should be commonly regulated by distinct chimeric EWS/ETS proteins. Indeed, several genes are common transcriptional targets of different chimeric EWS/ETS proteins in the murine system (11, 24, 35). Our data also showed that the 642 probes are coregulated in both EWS/FLI1-expressing cells and EWS/ERG-expressing cells. Further comparative studies of both the EWS/FLI1- and the EWS/ERG-mediated onset of EFT could allow us to understand the common functions of EWS/FLI1 and EWS/ERG in EFT. In addition, our systems are also useful for precisely distinguishing between the functions of these chimeric molecules in the development of EFT.

As mentioned above, the immunophenotypic analysis also revealed that the expression profiles of surface antigens in UET-13 cells were changed in favor of EFT cells in the presence of EWS/ETS (Fig. 4). Notably, the expression of CD54 (intercellular cell adhesion molecule-1 [ICAM1]), CD117 (c-kit), and CD271 (low-affinity nerve growth factor receptor [LNGFR]) increased in EWS/ETS-expressing UET-13 cells. These markers are positive in EFT cell lines (17, 28, 33), and in addition, CD117 is detected in about 40% of patient samples (17) and is negative in human primary MPCs (4, 43). Thus, it is reasonable to consider that a phenotypic marker of EFT was induced in UET-13 cells by EWS/ETS expression. On the other hand, CD54 and CD271 are positive in human primary MPCs (8, 25, 42), whereas these markers are negative in UET-13 cells. However, a previous report showed the disappearance of some positive markers, including CD271, from primary human MPCs during the process of ex vivo expansion

(25), and it has been speculated that the expression of these molecules in MPCs is induced in vivo via interaction with the bone marrow microenvironment and that the necessary stimuli are absent from ex vivo culture conditions. Therefore, the immunophenotype of UET-13 cells rather might be related to that of ex vivo-expanded primary human MPCs. In addition, it may be possible that EWS/ETS expression led to the reexpression of these disappeared markers in UET-13 cells without the necessary stimuli. In this case, the maintenance of CD271 expression outside of the bone marrow microenvironment might be a characteristic of EFT. Thus, our results proved that both EWS/FLI1 and EWS/ERG can be major causes of the expression of these markers and that human MPCs that precisely recapitulate the expression are strong candidates for the cell origins of EFT cells. The findings also imply that these antigens are suitable targets for diagnostic tools and new therapeutic agents. In fact, imatinib mesylate, which demonstrates anticancer activity against malignant cells expressing BCR-ABL as well as CD117 and platelet-derived growth factor receptor, inhibits proliferation and increases sensitivity to vincristine and doxorubicin in EFT cells (17).

Notably, our results also indicate that UET-13 cells, which have the MPC phenotype, possess the potential to acquire an EFT-like phenotype upon the expression of EWS/ETS. Unlike what is seen for human primary fibroblasts (31), ectopic EWS/ETS expression induces an EFT-like morphological change in human MPCs, suggesting that the cell type affects susceptibility to the events following EWS/ETS expression. In murine MPCs, retrovirally transduced EWS/FLI1 has been reported to induce the expression of CD99, a most useful marker for EFT, though the results are controversial (6, 45). However, our direct evidence obtained with UET-13 cells clearly demonstrated that CD99 expression is induced by EWS/ETS proteins in human MPCs. Moreover, we showed that the expression of CD99 might correlate with EWS/ETS-mediated morphological change, whereas the functional role of CD99 and the correlation between CD99 expression status and EWS/ETS-mediated morphological change in the development of EFT remain unclarified.

Consistent with the morphological and immunophenotypic changes, the expression pattern of a set of genes in EWS/ETS-expressing UET-13 cells shifted to that in EFT cells (Fig. 7C). Although EWS/ETS expression enhanced the ability of UET-13 cells to invade Matrigel, it did not promote migratory ability and surface-independent growth, as assessed by migration assay and soft agar colony formation assay (data not shown). We also failed to develop EFT-like tumors by injecting EWS/ETS-inducing UET-13 cells into irradiated nude mice treated with tetracycline (data not shown). These results imply that EWS/ETS expression is not sufficient to induce the full transformation in UET-13 cells, and other genetic abnormalities not regulated by EWS/ETS could still be required for the full transformation of human MPCs into EFT cells. An identification of these genes will greatly improve our understanding of the additional genetic lesions that occur after EWS/ETS expression. The genes expressed in EFT cell lines but not in EWS/ETS-expressing UET-13 cells would be candidates for such genes.

In summary, we reported the development of an inducible EWS/ETS expression system in UET-13 cells as a model for the development of EFT in MPCs. In our system, the chimeric genes alone are sufficient to confer EFT-like phenotypes, EFT-specific gene expression pattern, and partial but not full features of malignant transformation. Further analysis using our system should elucidate the pathogenic mechanism by which EFTs develop from MPCs, especially the initiating events mediated by EWS/ETS expression. Our system should also aid in the identification of novel targets of the EWS/ETS-mediated pathway as potential anticancer targets.

ACKNOWLEDGMENTS

This work was supported in part by health and labor sciences research grants (the 3rd-Term Comprehensive 10-Year Strategy for Cancer Control [H19-010], Research on Children and Families [H18-005 and H19-003], Research on Human Genome Tailor Made, and Research on Publicly Essential Drugs and Medical Devices [H18-005]) and a grant for child health and development from the Ministry of Health, Labor and Welfare of Japan, JSPS (Kakenhi 18790263). This work was also supported by a CREST, JST grant from the Japan Health Sciences Foundation for Research on Publicly Essential Drugs and Medical Devices and the Budget for Nuclear Research of the Ministry of Education, Culture, Sports, Science and Technology, based on screening and counseling by the Atomic Energy Commission. Y. Miyagawa is an awardee of a research resident fellowship from the Foundation for Promotion of Cancer Research (Japan) for the 3rd-Term Comprehensive 10-Year Strategy for Cancer Control.

We are grateful to T. Motoyama for the NRS-1 cell line. We respectfully thank S. Yamauchi for her secretarial work and M. Itagaki for many helpful discussions and support.

REFERENCES

1. **Akagi, T.** 2004. Oncogenic transformation of human cells: shortcomings of rodent model systems. Trends Mol. Med. **10**:542–548.
2. **Ambros, I. M., P. F. Ambros, S. Strehl, H. Kovar, H. Gadner, and M. Salzer-Kuntschik.** 1991. MIC2 is a specific marker for Ewing's sarcoma and peripheral primitive neuroectodermal tumors. Evidence for a common histogenesis of Ewing's sarcoma and peripheral primitive neuroectodermal tumors from MIC2 expression and specific chromosome aberration. Cancer **67**:1886–1893.
3. **Arvand, A., and C. T. Denny.** 2001. Biology of EWS/ETS fusions in Ewing's family tumors. Oncogene **20**:5747–5754.
4. **Bertani, N., P. Malatesta, G. Volpi, P. Sonego, and R. Perris.** 2005. Neurogenic potential of human mesenchymal stem cells revisited: analysis by immunostaining, time-lapse video and microarray. J. Cell Sci. **118**:3925–3936.
5. **Bloom, E. T.** 1972. Further definition by cytotoxicity tests of cell surface antigens of human sarcomas in culture. Cancer Res. **32**:960–967.
6. **Castillero-Trejo, Y., S. Eliazer, L. Xiang, J. A. Richardson, and R. L. Ilaria, Jr.** 2005. Expression of the EWS/FLI-1 oncogene in murine primary bone-derived cells results in EWS/FLI-1-dependent, Ewing sarcoma-like tumors. Cancer Res. **65**:8698–8705.
7. **Colter, D. C., I. Sekiya, and D. J. Prockop.** 2001. Identification of a subpopulation of rapidly self-renewing and multipotential adult stem cells in colonies of human marrow stromal cells. Proc. Natl. Acad. Sci. USA **98**: 7841–7845.
8. **Conget, P. A., and J. J. Minguell.** 1999. Phenotypical and functional properties of human bone marrow mesenchymal progenitor cells. J. Cell. Physiol. **181**:67–73.
9. **Davis, S., and P. S. Meltzer.** 2006. Ewing's sarcoma: general insights from a rare model. Cancer Cell **9**:331–332.
10. **Deneen, B., and C. T. Denny.** 2001. Loss of p16 pathways stabilizes EWS/FLI1 expression and complements EWS/FLI1 mediated transformation. Oncogene **20**:6731–6741.
11. **Deneen, B., S. M. Welford, T. Ho, F. Hernandez, I. Kurland, and C. T. Denny.** 2003. PIM3 proto-oncogene kinase is a common transcriptional target of divergent EWS/ETS oncoproteins. Mol. Cell. Biol. **23**:3897–3908.
12. **Eliazer, S., J. Spencer, D. Ye, E. Olson, and R. L. Ilaria, Jr.** 2003. Alteration of mesodermal cell differentiation by EWS/FLI-1, the oncogene implicated in Ewing's sarcoma. Mol. Cell. Biol. **23**:482–492.
13. **Fujii, Y., Y. Nakagawa, T. Hongo, Y. Igarashi, Y. Naito, and M. Maeda.** 1989. Cell line of small round cell tumor originating in the chest wall: W-ES. Hum. Cell **2**:190–191. (In Japanese.)
14. **Fukuma, M., H. Okita, J. Hata, and A. Umezawa.** 2003. Upregulation of Id2, an oncogenic helix-loop-helix protein, is mediated by the chimeric EWS/ets protein in Ewing sarcoma. Oncogene **22**:1–9.
15. **Gilbert, F., G. Balaban, P. Moorhead, D. Bianchi, and H. Schlesinger.** 1982.

Abnormalities of chromosome 1p in human neuroblastoma tumors and cell lines. Cancer Genet. Cytogenet. 7:33–42.
16. **Girish, V., and A. Vijayalakshmi.** 2004. Affordable image analysis using NIH Image/ImageJ. Indian J. Cancer **41**:47.
17. **Gonzalez, I., E. J. Andreu, A. Panizo, S. Inoges, A. Fontalba, J. L. Fernandez-Luna, M. Gaboli, L. Sierrasesumaga, S. Martin-Algarra, J. Pardo, F. Prosper, and E. de Alava.** 2004. Imatinib inhibits proliferation of Ewing tumor cells mediated by the stem cell factor/KIT receptor pathway, and sensitizes cells to vincristine and doxorubicin-induced apoptosis. Clin. Cancer Res. **10**:751–761.
18. **Hansen, M. B., S. E. Nielsen, and K. Berg.** 1989. Re-examination and further development of a precise and rapid dye method for measuring cell growth/cell kill. J. Immunol. Methods **119**:203–210.
19. **Hara, S., E. Ishii, S. Tanaka, J. Yokoyama, K. Katsumata, J. Fujimoto, and J. Hata.** 1989. A monoclonal antibody specifically reactive with Ewing's sarcoma. Br J. Cancer **60**:875–879.
20. **Hatori, M., H. Doi, M. Watanabe, H. Sasano, M. Hosaka, S. Kotajima, F. Urano, J. Hata, and S. Kokubun.** 2006. Establishment and characterization of a clonal human extraskeletal Ewing's sarcoma cell line, EES1. Tohoku J. Exp. Med. **210**:221–230.
21. **Homma, C., Y. Kaneko, K. Sekine, S. Hara, J. Hata, and M. Sakurai.** 1989. Establishment and characterization of a small round cell sarcoma cell line, SCCH-196, with t(11;22)(q24;q12). Jpn. J. Cancer Res. **80**:861–865.
22. **Hubert, R. S., I. Vivanco, E. Chen, S. Rastegar, K. Leong, S. C. Mitchell, R. Madraswala, Y. Zhou, J. Kuo, A. B. Raitano, A. Jakobovits, D. C. Saffran, and D. E. Afar.** 1999. STEAP: a prostate-specific cell-surface antigen highly expressed in human prostate tumors. Proc. Natl. Acad. Sci. USA **96**:14523–14528.
23. **Hu-Lieskovan, S., J. Zhang, L. Wu, H. Shimada, D. E. Schofield, and T. J. Triche.** 2005. EWS-FLI1 fusion protein up-regulates critical genes in neural crest development and is responsible for the observed phenotype of Ewing's family of tumors. Cancer Res. **65**:4633–4644.
24. **Im, Y. H., H. T. Kim, C. Lee, D. Poulin, S. Welford, P. H. Sorensen, C. T. Denny, and S. J. Kim.** 2000. EWS-FLI1, EWS-ERG, and EWS-ETV1 oncoproteins of Ewing tumor family all suppress transcription of transforming growth factor beta type II receptor gene. Cancer Res. **60**:1536–1540.
25. **Jones, E. A., S. E. Kinsey, A. English, R. A. Jones, L. Straszynski, D. M. Meredith, A. F. Markham, A. Jack, P. Emery, and D. McGonagle.** 2002. Isolation and characterization of bone marrow multipotential mesenchymal progenitor cells. Arthritis Rheum. **46**:3349–3360.
26. **Khoury, J. D.** 2005. Ewing sarcoma family of tumors. Adv. Anat. Pathol. **12**:212–220.
27. **Kiyokawa, N., Y. Kokai, K. Ishimoto, H. Fujita, J. Fujimoto, and J. I. Hata.** 1990. Characterization of the common acute lymphoblastic leukaemia antigen (CD10) as an activation molecule on mature human B cells. Clin. Exp. Immunol. **79**:322–327.
28. **Konemann, S., T. Bolling, A. Schuck, J. Malath, A. Kolkmeyer, K. Horn, D. Riesenbeck, S. Hesselmann, R. Diallo, J. Vormoor, and N. A. Willich.** 2003. Effect of radiation on Ewing tumour subpopulations characterized on a single-cell level: intracellular cytokine, immunophenotypic, DNA and apoptotic profile. Int. J. Radiat. Biol. **79**:181–192.
29. **Kovar, H., and A. Bernard.** 2006. CD99-positive "Ewing's sarcoma" from mouse bone marrow-derived mesenchymal progenitor cells? Cancer Res. **66**:9786.
30. **Kovar, H., M. Dworzak, S. Strehl, E. Schnell, I. M. Ambros, P. F. Ambros, and H. Gadner.** 1990. Overexpression of the pseudoautosomal gene MIC2 in Ewing's sarcoma and peripheral primitive neuroectodermal tumor. Oncogene **5**:1067–1070.
31. **Lessnick, S. L., C. S. Dacwag, and T. R. Golub.** 2002. The Ewing's sarcoma oncoprotein EWS/FLI induces a p53-dependent growth arrest in primary human fibroblasts. Cancer Cell **1**:393–401.
32. **Lin, P. P., R. I. Brody, A. C. Hamelin, J. E. Bradner, J. H. Healey, and M. Ladanyi.** 1999. Differential transactivation by alternative EWS-FLI1 fusion proteins correlates with clinical heterogeneity in Ewing's sarcoma. Cancer Res. **59**:1428–1432.
33. **Lipinski, M., K. Braham, I. Philip, J. Wiels, T. Philip, C. Goridis, G. M. Lenoir, and T. Tursz.** 1987. Neuroectoderm-associated antigens on Ewing's sarcoma cell lines. Cancer Res. **47**:183–187.
34. **Lochter, A., A. Srebrow, C. J. Sympson, N. Terracio, Z. Werb, and M. J. Bissell.** 1997. Misregulation of stromelysin-1 expression in mouse mammary tumor cells accompanies acquisition of stromelysin-1-dependent invasive properties. J. Biol. Chem. **272**:5007–5015.
35. **May, W. A., A. Arvand, A. D. Thompson, B. S. Braun, M. Wright, and C. T. Denny.** 1997. EWS/FLI1-induced manic fringe renders NIH 3T3 cells tumorigenic. Nat. Genet. **17**:495–497.
36. **May, W. A., S. L. Lessnick, B. S. Braun, M. Klemsz, B. C. Lewis, L. B. Lunsford, R. Hromas, and C. T. Denny.** 1993. The Ewing's sarcoma EWS/FLI-1 fusion gene encodes a more potent transcriptional activator and is a more powerful transforming gene than FLI-1. Mol. Cell. Biol. **13**:7393–7398.
37. **Miyagawa, Y., J. M. Lee, T. Maeda, K. Koga, Y. Kawaguchi, and T. Kusakabe.** 2005. Differential expression of a Bombyx mori AHA1 homologue during spermatogenesis. Insect Mol. Biol. **14**:245–253.
38. **Mori, T., T. Kiyono, H. Imabayashi, Y. Takeda, K. Tsuchiya, S. Miyoshi, H. Makino, K. Matsumoto, H. Saito, S. Ogawa, M. Sakamoto, J. Hata, and A. Umezawa.** 2005. Combination of hTERT and bmi-1, E6, or E7 induces prolongation of the life span of bone marrow stromal cells from an elderly donor without affecting their neurogenic potential. Mol. Cell. Biol. **25**:5183–5195.
39. **Nishimori, H., Y. Sasaki, K. Yoshida, H. Irifune, H. Zembutsu, T. Tanaka, T. Aoyama, T. Hosaka, S. Kawaguchi, T. Wada, J. Hata, J. Toguchida, Y. Nakamura, and T. Tokino.** 2002. The Id2 gene is a novel target of transcriptional activation by EWS-ETS fusion proteins in Ewing family tumors. Oncogene **21**:8302–8309.
40. **Ogose, A., T. Motoyama, T. Hotta, and H. Watanabe.** 1995. In vitro differentiation and proliferation in a newly established human rhabdomyosarcoma cell line. Virchows Arch. **426**:385–391.
41. **Prieur, A., F. Tirode, P. Cohen, and O. Delattre.** 2004. EWS/FLI-1 silencing and gene profiling of Ewing cells reveal downstream oncogenic pathways and a crucial role for repression of insulin-like growth factor binding protein 3. Mol. Cell. Biol. **24**:7275–7283.
42. **Quirici, N., D. Soligo, P. Bossolasco, F. Servida, C. Lumini, and G. L. Deliliers.** 2002. Isolation of bone marrow mesenchymal stem cells by anti-nerve growth factor receptor antibodies. Exp. Hematol. **30**:783–791.
43. **Reyes, M., T. Lund, T. Lenvik, D. Aguiar, L. Koodie, and C. M. Verfaillie.** 2001. Purification and ex vivo expansion of postnatal human marrow mesodermal progenitor cells. Blood **98**:2615–2625.
44. **Reyes, M., and C. M. Verfaillie.** 2001. Characterization of multipotent adult progenitor cells, a subpopulation of mesenchymal stem cells. Ann. N. Y. Acad. Sci. **938**:231–235.
45. **Riggi, N., L. Cironi, P. Provero, M. L. Suva, K. Kaloulis, C. Garcia-Echeverria, F. Hoffmann, A. Trumpp, and I. Stamenkovic.** 2005. Development of Ewing's sarcoma from primary bone marrow-derived mesenchymal progenitor cells. Cancer Res. **65**:11459–11468.
46. **Riggi, N., M. L. Suva, and I. Stamenkovic.** 2006. Ewing's sarcoma-like tumors originate from EWS-FLI-1-expressing mesenchymal progenitor cells. Cancer Res. **66**:9786.
47. **Sekiguchi, M., T. Oota, K. Sakakibara, N. Inui, and G. Fujii.** 1979. Establishment and characterization of a human neuroblastoma cell line in tissue culture. Jpn. J. Exp. Med. **49**:67–83.
48. **Smith, R., L. A. Owen, D. J. Trem, J. S. Wong, J. S. Whangbo, T. R. Golub, and S. L. Lessnick.** 2006. Expression profiling of EWS/FLI identifies NKX2.2 as a critical target gene in Ewing's sarcoma. Cancer Cell **9**:405–416.
49. **Staege, M. S., C. Hutter, I. Neumann, S. Foja, U. E. Hattenhorst, G. Hansen, D. Afar, and S. E. Burdach.** 2004. DNA microarrays reveal relationship of Ewing family tumors to both endothelial and fetal neural crest-derived cells and define novel targets. Cancer Res. **64**:8213–8221.
50. **Takeda, Y., T. Mori, H. Imabayashi, T. Kiyono, S. Gojo, S. Miyoshi, N. Hida, M. Ita, K. Segawa, S. Ogawa, M. Sakamoto, S. Nakamura, and A. Umezawa.** 2004. Can the life span of human marrow stromal cells be prolonged by bmi-1, E6, E7, and/or telomerase without affecting cardiomyogenic differentiation? J. Gene Med. **6**:833–845.
51. **Tondreau, T., N. Meuleman, A. Delforge, M. Dejeneffe, R. Leroy, M. Massy, C. Mortier, D. Bron, and L. Lagneaux.** 2005. Mesenchymal stem cells derived from CD133-positive cells in mobilized peripheral blood and cord blood: proliferation, Oct4 expression, and plasticity. Stem Cells **23**:1105–1112.
52. **Torchia, E. C., S. Jaishankar, and S. J. Baker.** 2003. Ewing tumor fusion proteins block the differentiation of pluripotent marrow stromal cells. Cancer Res. **63**:3464–3468.
53. **Woodbury, D., E. J. Schwarz, D. J. Prockop, and I. B. Black.** 2000. Adult rat and human bone marrow stromal cells differentiate into neurons. J. Neurosci. Res. **61**:364–370.

0013-7227/08/$15.00/0
Printed in U.S.A.

Endocrinology 149(4):1786–1792

doi: 10.1210/en.2007-1015

Cyp11b1 Is Induced in the Murine Gonad by Luteinizing Hormone/Human Chorionic Gonadotropin and Involved in the Production of 11-Ketotestosterone, a Major Fish Androgen: Conservation and Evolution of the Androgen Metabolic Pathway

Takashi Yazawa, Miki Uesaka, Yoshihiko Inaoka, Tetsuya Mizutani, Toshio Sekiguchi, Takashi Kajitani, Takeshi Kitano, Akihiro Umezawa, and Kaoru Miyamoto

Department of Biochemistry (T.Y., M.U., Y.I., T.M., T.S., T.Ka., K.M.), Faculty of Medical Sciences, University of Fukui, Fukui 910-1193, Japan; Department of Materials and Life Science (T.Ki.), Graduate School of Science and Technology, Kumamoto University, Kumamoto 860-8555, Japan; and National Research Institute for Child Health and Development (A.U.), Tokyo 157-8535, Japan

We have shown previously that Cyp11b1, an 11β-hydroxylase responsible for glucocorticoid biosynthesis in the adrenal gland, was induced by cAMP in androgen-producing Leydig-like cells derived from mesenchymal stem cells. We found that Cyp11b1 was induced in male Leydig cells, or female theca cells, when human chorionic gonadotropin was administered in immature mice. Expression of Cyp11b1 in rodent gonads caused the production of 11-ketotestosterone (11-KT), a major fish androgen, which induces male differentiation or spermatogenesis in fish. As in teleosts, plasma concentrations of 11-KT were elevated in human chorionic gonadotropin-treated mice. In contrast to teleosts, however, plasma concentrations of 11-KT were similar in both sexes, despite levels of testosterone, a precursor substrate, being about 20 times higher in male mice. Because expression of 11β-hydroxysteroid dehydrogenase type 2, was much higher in the mouse ovary than in the testis, conversion of testosterone into 11-KT may occur more efficiently in the ovary. In a luciferase reporter system that was responsive to and activated by androgens, 11-KT efficiently activated mammalian androgen receptor-mediated transactivation. Our results suggest that the androgen metabolic pathway is conserved between teleosts and mammals, despite sexual dominance and reproductive functions of 11-KT being altered during evolution. (*Endocrinology* 149: 1786–1792, 2008)

A MEMBER OF the cytochrome P-450 superfamily, steroid 11β-monooxygenase (CYP11B1 in humans or Cyp11b1 in rodents), is responsible for the last step of glucocorticoid biosynthesis in mammalian adrenal cortices. The enzyme has been shown to function in the zona fasciculate-reticularis of the adrenal cortex by an ACTH-regulated manner but has not generally been thought to work in the gonad (1, 2). Wang *et al.* (3), however, reported that Cyp11b1 is expressed in rat Leydig cells and involved in the regulation of 11β-hydroxysteroid dehydrogenase (11β-HSD) activity by producing 11β-hydroxysteroid. In addition to the adrenal (head kidney), fish steroid 11β-hydroxylase, a homolog of Cyp11b1, is expressed in testicular Leydig cells to produce 11-ketotstosterone (11-KT), a major androgen in fishes, with the aid of 11β-HSD (4, 5). 11-KT is necessary for inducing the male sexual phenotype and spermatogenesis in many teleost species (6–10). Although Cyp11b1 knockout (KO) mice are not reported until now, congenital adrenal hyperplasia with various abnormalities in gonad was reported for human CYP11B1 mutations (11, 12).

Two isoforms of 11β-HSD have been characterized in mammals and thought to be involved in the glucocorticoid metabolism (13, 14). Type I enzyme (11β-HSD1) acts predominantly as a reductase of 11-ketosteroids, whereas type II enzyme mainly acts as an oxidase of 11-hydroxysteroids. 11β-HSD1 is an oxidation of nicotinamide adenine dinucleotide phosphate-dependent oxidoreductase in key glucocorticoid target tissues such as liver, gonads, and adipose tissue, converting cortisone to cortisol, thereby regulating the level of active glucocorticoid available for intracellular glucocorticoid receptors. Deficiency of 11β-HSD1 is the cause of apparent cortisone reductase deficiency. In some cases, it may be associated with polycystic ovary syndrome by adrenal androgen excess (15, 16), although results are controversial (17, 18). By contrast, the type 2 enzyme (11β-HSD2) is an oxidation of nicotinamide adenine dinucleotide-dependent dehydrogenase found predominantly in mineralocorticoid-responsive tissues such as the kidney, salivary glands, and colon. In these tissues, 11β-HSD2 converts cortisol to cortisone or corticosterone to 11-dehydrocorticosterone, thereby protecting mineralocorticoid receptors from inappropriate

First Published Online December 27, 2007

Abbreviations: AR, Androgen receptor; ArKO, androgen receptor KO; DHT, dihydrotestosterone; Gapdh, glyceraldehyde-3-phosphate dehydrogenase; hCG, human chorionic gonadotropin; 11β-HSD, 11β-hydroxysteroid dehydrogenase; 11β-HSD1, type I enzyme 11β-HSD; 11β-HSD2, type 2 enzyme 11β-HSD; KO, knockout; 11-KT, 11-ketotstosterone; MSC, mesenchymal stem cell; SF-1, steroidogenic factor 1.

Endocrinology is published monthly by The Endocrine Society (http://www.endo-society.org), the foremost professional society serving the endocrine community.

occupation by cortisol. Mutations in the 11β-HSD2 gene cause a rare monogenic juvenile hypertensive syndrome called apparent mineralocorticoid excess. About half of the Hsd11b2 KO mice die within 48 h after birth (19). Although survivors were fertile, they showed human apparent mineralocorticoid excess-like phenotype. Analysis of litter size or their gonadal functions, however, have not been reported yet.

In teleosts, 11β-HSD2 is abundantly expressed in testicular Leydig cells and plays a role in the final step of production of 11-KT, a major fish androgen (20, 21).

In this study, we report induction of Cyp11b1 and production of 11-KT in murine gonads by human chorionic gonadotropin (hCG) stimulation. We also show that, in contrast to teleosts, expression of 11β-HSD2 was much higher in the mouse ovary than the testis. Although the metabolic pathway of 11-KT production is conserved between teleosts and mammals, the roles of 11-KT may be different between them.

Materials and Methods

Animals and hormone assay

Immature C57BL/6J mice (21–28 d old) were purchased from Charles River (Wilmington, MA). At all times, animals were treated according to National Institutes of Health guidelines. Animals were treated ip with 10 U hCG (Teikoku Zouki, Tokyo, Japan) or 5 U ACTH (Sigma, St. Louis, MO). At each time point, animals were anesthetized with diethyl ether. After collection of serum samples, concentrations of serum steroids were determined by ELISA (Cayman Chemical Co., Ann Arbor, MI). Cross-reactivities of other steroids in these assays were as follows: testosterone [5α-dihydrotestosterone (DHT), 27.4%; 5β-DHT, 18.9%; androstenedione, 3.7%; 11-KT, 2.2%; 5-androsteneodiol, 0.51%], 11-KT (4-androsten-11β, 17β-diol-3one, 0.01%).

Plasmids

A ARE-Luc reporter and hAR/pSG5 were kindly provided by Dr. Shigeaki Kato (The University of Tokyo, Tokyo, Japan). AR/pcDNA3.1 was kindly provided by Dr. Makoto Nakai (Chemicals Assessment Center, Chemicals Evaluation and Research Institute, Saitama, Japan). The slp-ARU-tk/Luc was made by inserting the oligonucleotides of the mouse sex-limited protein upstream androgen-responsive unit in the tk/Luc plasmid (22).

RT-PCR

Total RNA from cultured cells was extracted using Trizol reagent (Invitrogen Corp., Carlsbad, CA). RT-PCR was performed as described previously (23). The reaction products of the RT-PCR assay were subjected to electrophoresis in a 1.5% agar gel, and the resulting bands were visualized by staining with ethidium bromide. The primers used for PCR were as follows: Hsd11b1 (forward, ttatgaaaaaatacctcctccc, reverse, cttgatctccagggcgcattc), Hsd11b2 (forward, aaggcagaggcatcagccgt, reverse, tgccattctgagtgaattcag), aldo-keto-reductase 1b7 (Akr1b7, forward, tcactcagagaactctctgc, reverse, atcatgcacggatctcatca). The primers used for other genes were as described by Yazawa *et al.* (23).

Cell culture, transfection, and luciferase assay

MA10 cells (kindly provided by Dr. Mario Ascoli, University of Iowa, Iowa City, IA) were cultured in Waymouth 752 supplemented with 15% horse serum. CV-1 and KUM9 cells were cultured in DMEM with 10% fetal calf serum. KGN cells (kindly gifted by Dr. Toshihiko Yanase, Kyushu University, Fukuoka, Japan) were culture in the DMEM/F-12 medium with 10% fetal calf serum. Transfection and luciferase reporter assays were performed as described before (24). After 24 h of transfection, the cells were treated with vehicle, androgens (Sigma), with or without aromatase inhibitors, fadrozole (Ciba Geigy Ltd., Basel, Switzerland), or anastrozole (Astra Zeneca Pharmaceuticals, Macclesfield, UK) for 24 h. Data presented represent the mean of at least four independent experiments.

Western blot analysis

The extraction of protein from the cultured cells and subsequent quantification was performed as described previously (23, 24). Equal amounts of proteins (50 μg) were analyzed by 10% SDS-PAGE and transferred to polyvinylidene difluoride membranes. Western blot analyses of Cyp11b1, Hsd11b2, glyceraldehyde-3-phosphate dehydrogenase (Gapdh), and β-tubulin were carried out with antiserum directed against Cyp11b1 (kindly given by Dr. Hiroshi Takemori, University of Osaka, Osaka, Japan), Hsd11b2 (Chemicon International, Inc., Temecula, CA), Gapdh (6C5; Santa Cruz Biotechnology, Santa Cruz, CA), and β-tubulin (D-10; Santa Cruz Biotechnology). ECL Western blot reagents (Amersham Pharmacia Biotech, Piscataway, NJ) were used for detection.

Immunohistochemistry

Tissue treatment and immunohistochemistry were performed as described previously (25). Briefly, gonads were fixed in 4% paraformaldehyde solution, dehydrated in a graded ethanol series, and embedded in paraffin wax. Sections of 7 μm thickness were treated with anti-Cyp11b1 or anti-Hsd11b2 antibodies and developed using a Vectastain Elite ABC kit (Vector Laboratories, Burlingame, CA).

Statistics

Data from transactivation experiments were analyzed by the Student's *t* test. $P < 0.01$ was considered statistically significant.

Results

Expression of Cyp11b1 in murine gonads

In a previous study, we made testosterone-producing adult Leydig-like cells from murine bone marrow-derived mesenchymal stem cells, KUM9 (23). A peculiar phenomenon that occurred in these cells was that Cyp11b1, an adrenal-specific gene, was induced by cAMP treatment after 5 d (Fig. 1A). Cyp11b1 mRNA and proteins were also induced in Leydig cell tumor derived-MA10 cells at 2 h after cAMP treatments, increasing thereafter (Fig. 1, B and C). In contrast, Cyp11b2 was not induced in both cells (Fig. 1, A and B).

To investigate the physiological relevance of these phenomena, we treated immature mice with hCG. Although Cyp11b1 mRNA and proteins were never detected before the hCG treatment, they were induced by hCG treatment both in the male and female gonad within 6 h (Fig. 2, A and B). The expression was continued for at least 48 h, although testicular levels were decreased at 48 h. In contrast, ACTH treatment did not induce gonadal Cyp11b1 mRNA, despite the fact that it induced adrenal ACTH-inducible gene, Akr1b7 mRNA (Fig. 1C). Immunohistochemistry showed that Cyp11b1 proteins were induced in the testicular Leydig cells and the ovarian theca cells (Fig. 2, C–F). The expression of Cyp11b2 was never detected.

Fish androgen, 11-KT, production in the murine gonad

Teleost 11β-hydroxylase, CYP11B, is also induced by hCG treatment in immature eel Leydig cells (4). This causes the production of fish androgen, 11-KT, and premature spermatogenesis (26). To determine whether a similar phenomenon occurs in murine gonads, we measured the plasma androgen levels in the hCG-treated mice (Fig. 3). hCG treatment elevated the plasma testosterone levels in males and

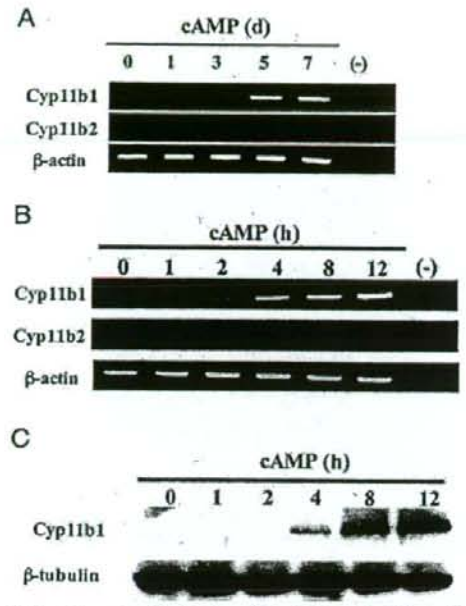

FIG. 1. Time-dependent induction of Cyp11b1 mRNA (A and B) and protein (C) by cAMP in mesenchymal stem cells (A) and MA10 cells (B and C). A, Murine mesenchymal stem cells stably transfected with an SF-1-expression vector were cultured and treated with 8-bromoadenosine-cAMP for the indicated times. mRNA levels of each gene were analyzed by RT-PCR. B and C, MA10 cells were treated with cAMP for the indicated times. C, Western blot analyses were performed with antibodies against Cyp11b1 and β-tubulin using the same lysates.

females, with much higher concentrations in the males at all times (0, 24, 48 h). The hCG treatment also elevated the 11-KT levels, but surprisingly, they were almost the same in both sexes. Thus, much higher conversion of 11-KT from testosterone seemed to occur in the ovary.

After the 11β-hydroxylation, 11-KT is produced by the actions of 11β-HSD (Fig. 4A). Two isoforms of 11β-HSD exist in mammals and have reverse activity *in vivo*; type I enzyme dominantly acts as a reductase and type II exhibits only an oxidative activity. It is possible that the expression pattern of the two isoforms in gonads may determine sexual dimorphism with respect to the conversion of testosterone to 11-KT. Therefore, we investigated the expression of the 11β-HSDs in the testis and ovary (Fig. 4B). In contrast to Cyp11b1, expression levels of 11β-HSDs, Hsd11b1 and Hsd11b2, were not affected by the hCG treatment. Hsd11b1 mRNA was expressed at higher levels in the testis than the ovary, whereas Hsd11b2 mRNA was expressed at very high levels in the ovary as reported previously (13). Only ovarian Hsd11b2 protein was detected by Western blot analysis (Fig. 4C). Immunohistochemistry showed that Hsd11b2 protein was expressed mainly in the theca cells (Fig. 4D). Using the same antibody, specific staining was not detected in the testis (data not shown). These results indicate that sexual dimorphic expression of Hsd11b2 enzyme causes the higher conversion of testosterone into 11-KT in the female.

The effects of 11-KT and other androgen on androgen receptor (AR) activation

To investigate whether 11-KT is an effective ligand of mammalian AR, we compared the androgen-dependent transcriptional activity of 11-KT with various androgens using the luciferase reporter system (Fig. 5). DHT activated AR-mediated transcription in a dose-dependent manner from 10^{-10} M. 11-KT was as effectively strong as testosterone, although to a lesser extent than DHT. Androstenedione and 11OH-testosterone were the poor activators.

AR is exclusively expressed in the granulosa cells in the ovary (27). Because androgens can be converted to estrogens by aromatase, they could act as not only androgen but also the precursors of estrogens in these cells. Therefore, we compared androgenic activity of the aromatizable testosterone with that of the nonaromatizable 11-KT by their transcriptional activities through AR in the granulosa-like tumor KGN cells (Fig. 6). Both androgens significantly activated the AR-mediated transcription from 10^{-10} M in these cells. However, 11-KT showed significant higher activity than testosterone at 10^{-10} and 10^{-9} M ($P < 0.01$). Such a difference was blunted by the addition of aromatase inhibitors, fadrozole (Fig. 6) or anastrozole (data not shown). A significant difference was not observed at 10^{-8} M, probably because unconverted testosterone levels were high enough to exert the maximum response at this concentration. These results suggest that the conversion from testosterone to 11-KT may have a role in maintaining the androgenic activity caused by testosterone in granulosa cells by preventing aromatization.

Discussion

In this study, we demonstrated that the metabolic pathway producing 11-KT in the fish gonad is also conserved in murine gonads, although there is a marked difference in the production pattern in the gonads. In fish, this pathway is dominant in males (testis) and causes much higher 11-KT levels when compared with females. 11-KT is necessary for the male sexual phenotype and spermatogenesis in fish testis. In addition, it induces female-to-male sex reversal in some teleost species (9, 10). In contrast to fish, this pathway is dominant in female (ovary) mice.

In mammals, it is believed that the steroid 11β-hydroxylase, CYP11B1 or Cyp11b1, is an adrenal-specific gene and is responsible for the last step of glucocorticoid biosynthesis. However, Cyp11b1 was induced by cAMP treatment in the Leydig-like cells made from murine bone marrow-derived mesenchymal stem cells as well as in Leydig cell tumor-derived MA10 cells. Supporting the physiological relevance of this phenomenon, it was also induced *in vivo* by hCG treatment in testicular Leydig cells and ovarian theca cells. In addition, Wang *et al.* (3) reported that Cyp11b1 was expressed in rat testis. These results indicate that 11β-hydroxylase (Cyp11b1) is not an adrenal-specific gene. Recently Val *et al.* (28) reported that adrenal-like cells exist in the embryonic murine testis, and they respond to both ACTH and hCG that leads to the expression of Cyp11b1. However, it is unlikely that adrenal-like cells in murine gonads can explain our present observation because adrenal-like cells are presently unknown in the murine ovary, and induction of

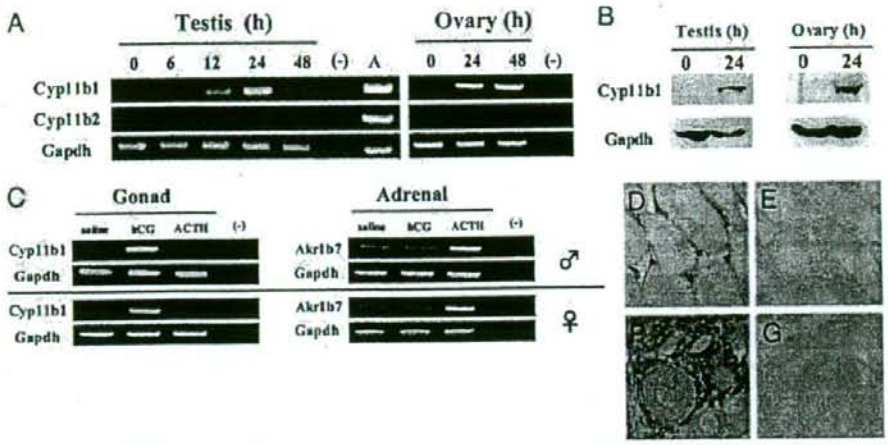

FIG. 2. Induction of Cyp11b1 mRNA and protein by hCG in murine testes and ovaries. Animals were treated with hCG, and gonads were removed at indicated times (A and B). A, mRNA levels of each gene were analyzed by RT-PCR. Lane A represents an adrenal. B, Western blot analyses were performed with antibodies against Cyp11b1 and Gapdh using the same lysates. C, Animals were treated with saline, hCG, or ACTH, and tissues were removed at 16 h. mRNA levels of each gene were analyzed by RT-PCR. D–G, Localization of Cyp11b1 protein in the murine gonad. Testes or ovaries from mice treated with hCG for 24 h were used. Positive staining for Cyp11b1 was observed in testicular Leydig cells (D) and ovarian theca cells (F). No staining was observed in control sections incubated with nonimmune serum (E and G).

Cyp11b1 was observed in almost all populations of Leydig or theca cells. In addition, Cyp11b1 mRNA was not detected in gonads of ACTH-treated animals because O'Shaughnessy *et al.* (29) reported the deficiency of response to ACTH stimulation in adult Leydig cells. Rather, these results suggest that testicular Leydig cells and ovarian theca cells have a capacity to express Cyp11b1, as in the case of adrenal-like cells.

As we reported previously (23), much longer times (1–5 d) were necessary to induce all the steroidogenic enzymes by cAMP treatment in mesenchymal stem cells (MSCs) (including KUM9) than steroidogenic cell lines including MA10 (1–8 h). Then we speculated that the cAMP treatment in MSCs induced the differentiation of stem cells into steroidogenic linage in MSCs, whereas it induces the transactivation of steroidogenic enzymes in steroidogenic cell lines. Supporting this assumption, Cyp11b1 had been induced by retreatment of the cAMP in MSC-derived cells as fast as in the MA10 cells after 7 d cAMP treatment and ensuring depletion of the cAMP.

Considerable work has been done on the mechanisms that regulate transcription of human and bovine 11β-hydroxylase genes, CYP11B1 and CYP11B, respectively. Transcription factors, steroidogenic factor 1 (SF-1) (also known as Ad4BP) and cAMP response element-binding protein are known to play a vital role in both species (30–32). The model also seems to be applicable to the transcriptional regulation of murine Cyp11b1 because it is induced in nonsteroidogenic mesenchymal stem cells by the stable transfection of SF-1 and the treatment of cAMP (23, 33), although its promoter analysis is not yet reported. SF-1 is essential for the development of the adrenal gland and gonad and sexual differentiation (34–36). It is expressed in the adrenal cortex, testicular Leydig and Sertoli cells, ovarian theca and granulosa cells, pituitary gonadotroph, hypothalamus, and spleen. SF-1 is a member of the nuclear receptor superfamily and regulates the cell-specific expression of a variety of different genes involved in steroidogenesis including a number of steroid hydroxylases (34–37). The expression pattern of SF-1 during urogenital development suggested that adrenal and gonadal cells are derived from common precursor cell populations (38). Therefore, it is conceivable that Cyp11b1 mRNA is induced by LH/hCG treatment in gonadal steroidogenic cells as well as by ACTH treatment in the adrenal gland. However, other adrenal-specific factors should be involved in the transcription of Cyp11b1 because the expression levels were much higher in adrenocortical cells than gonadal cells, even after hCG or cAMP treatment. Further studies will be necessary to understand the regulatory mechanisms of the Cyp11b1 gene expression.

Because the substrate precursors for glucocorticoid are not produced in the gonad due to the deficiency of Cyp21, Cyp11b1 may be involved in steroid metabolism, other than glucocorticoid synthesis in the gonad. In eel testis, 11β-hydroxylase is induced by hCG treatment and contributes to the production of the fish androgen 11-KT (4, 26). This was also observed in murine gonads, with the elevation of the plasma 11-KT levels by hCG treatment. It is likely that 11-KT is not only a teleost androgen but also a mammalian androgen. This is supported by the findings that 11-KT was able to activate mammalian AR-mediated transcription.

There is, however, a marked difference between teleosts and mammals with respect to the production of 11KT. 11-KT is a major androgen in most male teleost species and was found at much higher concentrations in male plasma than in female, whereas this is usually not the case for testosterone (39, 40). In teleosts, 11-KT is involved in the many male reproductive processes, such as spermatogenesis (6, 7), development of secondary sex characteristics (8, 9), and modulation of behavior (9). In addition, it eventually induces

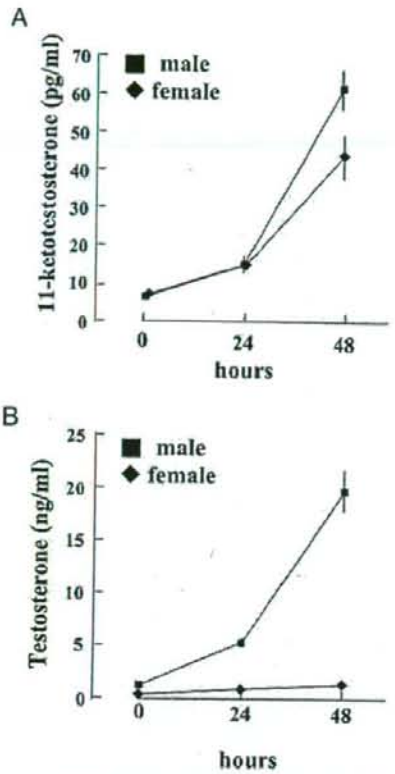

FIG. 3. Concentrations of serum androgens in mice treated with hCG. Serum 11-KT (A) and testosterone (B) concentrations in male (■) and female (◆) mice treated with hCG at indicated times. Data for each point are from five animals (means and SEM).

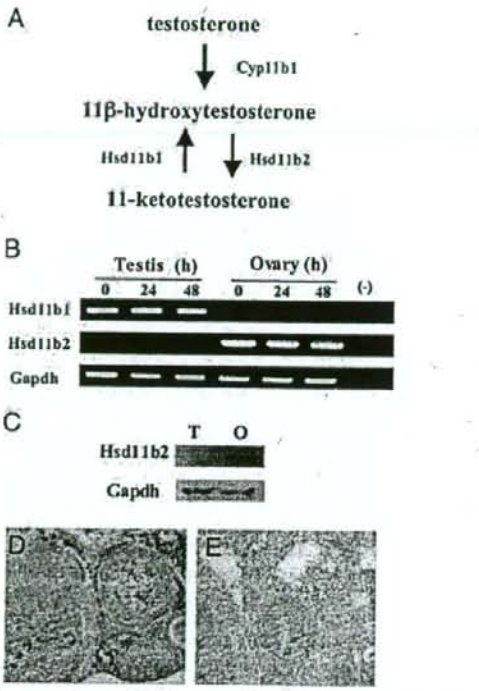

FIG. 4. The expression and localization of the 11β-HSDs in the murine gonad. A, The enzymes and pathways involved in the synthesis of 11-KT. B, mRNA levels of each gene in gonads treated with hCG for indicated times were analyzed by RT-PCR. C, Immunoblot of Hsd11b2 and Gapdh proteins in testis (T) and ovary (O) using the same lysates. Localization of Hsd11b2 protein in the ovary (D and E). Positive staining for Hsd11b2 was observed in theca cells (D). No staining was observed in control sections incubated with nonimmune serum (E).

female-to-male sex reversal in some species (10). In contrast to teleosts, murine plasma 11-KT concentrations were at similar levels in both sexes, whereas testosterone levels were much higher in males. Such a difference between these vertebrates implies a difference in sexual dimorphic expression of the enzymes involving the conversion of 11-KT in their gonads. In teleost gonads, P450 11β is exclusively expressed in the testis (41–43), whereas murine Cyp11b1 was induced by hCG both in the testis and ovary at similar levels. By contrast, teleost 11β-HSD2 is abundantly expressed in the testis (20, 21), whereas murine Hsd11b2 was expressed more highly in the ovary. These results indicate that the 11-KT production pathway is conserved between teleosts and mammals, although its major physiological role(s) may have become different during their evolution.

Wang *et al.* (3) reported that 11β-hydroxysteroids or 11-ketosteroids were involved in the regulation of 11β-HSD activity in Leydig cells. 11β-hydroxysteroids were efficient inhibitors of Hsd11b1 dehydrogenase activity, whereas 11-keto compounds were effective as inhibitors of oxidoreductase activity. 11β-HSDs in Leydig cells convert active glucocorticoids to the inert 11-keto form, thereby playing a protective role in blunting the suppressive effects of glucocorticoid on Leydig cell steroidogenesis. Therefore, 11-KT is a possible controller of the testicular steroidogenesis via regulating the activity of 11β-HSDs. This may also be true in the ovarian steroidogenesis. As in the case of testicular Leydig cells, ovarian steroidogenesis is also inhibited by glu-

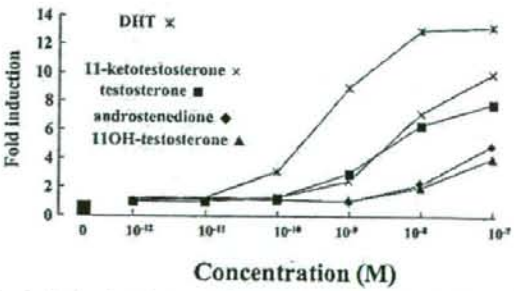

FIG. 5. Activation of mammalian AR by various androgens. CV-1 cells were transiently transfected with the ARE-Luc vector together with an AR expression vector. After 24 h after transfection, cells were incubated with or without increasing concentrations of various androgens for 24 h. Data are shown as the mean ± SEM values of at least four independent assays.

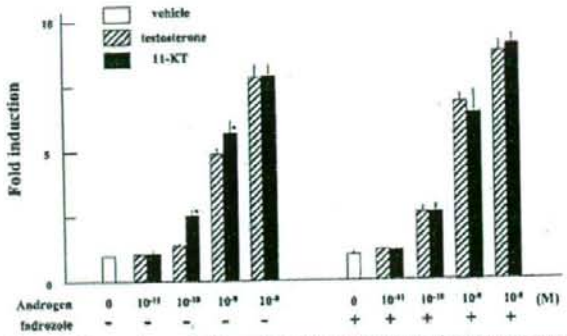

FIG. 6. Comparison of AR-mediated transactivation by testosterone and 11-KT in granulosa like-tumor KGN cells. KGN cells were transiently transfected with the slp-ARU-tk/Luc vector together with an AR expression vector. After 24 h after transfection, cells were incubated with or without androgens and fadrozole (1 μM) for 24 h. Data are shown as the mean ± SEM values of at least four independent assays. *, Significant difference in transactivation between testosterone and 11-KT ($P < 0.01$).

cocorticoid (44, 45). In addition, higher expression of Hsd11b2 in the ovary suggests that ovarian Hsd11b2 may regulate the ovarian steroidogenesis by limiting the accessibility of active glucocorticoid to ovarian glucocorticoid receptors via 11-KT production. It also suggests that the ovary may be a new target organ of the mineralocorticoid-mineralocorticoid receptor pathway. Recently Fru *et al.* (46) reported that, compared with the glucocorticoid actions, mineralocorticoid stimulates progesterone synthesis by periovulatory granulosa cells in macaques. Therefore, it is conceivable that the complex steroid metabolism and signaling including androgen may regulate ovarian steroidogenesis.

The induction of 11KT by gonadotropin treatment suggests that 11-KT is also involved in folliculogenesis. In fact, androgen receptor KO (ArKO) female mice showed a subfertile phenotype, resulting from the impairment of ovulation and corpus lutea formation (27, 47). Because ovarian AR is exclusively expressed in granulosa cells (27), those phenotypes in ArKO mice suggest that androgens induce genes associated with folliculogenesis in granulosa cells. Our results in KGN cells suggest that conversion from testosterone to 11-KT may have a role in maintaining the androgenic activity caused by testosterone in granulose cells because it can efficiently induce AR-regulated genes in these cells. Shiina *et al.* (27) reported that Kit ligand is the direct downstream target of AR, and its down-regulation in ArKO mice is the cause of premature ovarian failure. Future studies will be necessary to investigate the relationship between Kit ligand and 11-KT-AR pathway in the ovary.

In summary, we reported that the metabolic pathway producing 11-KT, a major teleost androgen, was conserved in the mammalian gonad, although it was more active in the ovary. In female eels, however, 11-KT synthesis and levels fluctuated during oogenesis and follicular maturation (48). Therefore, 11-KT production and AR signaling in female might be conserved from teleosts to mammals, even though 11-KT has been replaced by DHT in male during evolution.

Acknowledgments

We are grateful to Drs. S. Kato, M. Nakai, H. Takemori, T. Yanase, and M. Ascoli for providing the materials. We also thank Ms. Y. Inoue, K. Matsuura, and H. Fujii for technical assistance.

Received July 24, 2007. Accepted December 19, 2007.

Address all correspondence and requests for reprints to: Kaoru Miyamoto, Department of Biochemistry, Faculty of Medical Sciences, University of Fukui, Shimoaizuki, Matsuoka, Eiheiji-cho, Fukui 910-1193, Japan. E-mail: kmiyamot@u-fukui.ac.jp.

This work was supported in part by a grant from the Smoking Research Foundation, Kanzawa Medical Research Foundation, 21st Century Center of Excellence Program (Medical Science), and Research and Education Program for Life Science.

Disclosure Statement: All authors (T.Y., M.U., Y.I., T.M., T.S., T.Ka., T.Ki., A.U., K.M.) have nothing to declare.

References

1. **Domalik LJ, Chaplin DD, Kirkman MS, Wu RC, Liu WW, Howard TA, Seldin MF, Parker KL** 1991 Different isozymes of mouse 11β-hydroxylase produce mineralocorticoids and glucocorticoids. Mol Endocrinol 5:1853–1861
2. **Ogishima T, Suzuki H, Hata J, Mitani F, Ishimura Y** 1992 Zone-specific expression of aldosterone synthase cytochrome P-450 and cytochrome P-45011β in rat adrenal cortex: histochemical basis for the functional zonation. Endocrinology 130:2971–2977
3. **Wang GM, Ge RS, Latif SA, Morris DJ, Hardy MP** 2002 Expression of 11β-hydroxylase in rat Leydig cells. Endocrinology 143:621–626
4. **Jiang JQ, Kobayashi T, Ge W, Kobayashi H, Tanaka M, Okamoto M, Nonaka Y, Nagahama Y** 1996 Fish testicular 11β-hydroxylase: cDNA cloning and mRNA expression during spermatogenesis. FEBS Lett 397:250–252
5. **Jiang JQ, Young G, Kobayashi T, Nagahama Y** 1998 Eel (*Anguilla japonica*) testis 11β-hydroxylase gene is expressed in interrenal tissue and its product lacks aldosterone synthesizing activity. Mol Cell Endocrinol 146:207–211
6. **Miura T, Yamauchi K, Takahashi H, Nagahama Y** 1991 Hormonal induction of all stages of spermatogenesis *in vitro* in the male Japanese eel (*Anguilla japonica*). Proc Natl Acad Sci USA 88:5774–5778
7. **Nagahama Y** 1994 Endocrine regulation of gametogenesis in fish. Int J Dev Biol 38:217–229
8. **Mayer I, Borg B, Schulz R** 1990 Seasonal changes in and effect of castration/androgen replacement on the plasma levels of five androgens in the male three-spined stickleback, *Gasterosteus aculeatus L.* Gen Comp Endocrinol 79:23–30
9. **Kobayashi M, Nakanishi T** 1999 11-Ketotestosterone induces male-type sexual behavior and gonadotropin secretion in gynogenetic crucian carp, *Carassius auratus langsdorfii*. Gen Comp Endocrinol 115:178–187
10. **Cardwell JR, Liley NR** 1991 Hormonal control of sex and color change in the stoplight parrotfish, *Sparisoma viride*. Gen Comp Endocrinol 81:7–20
11. **Curnow KM, Slutsker L, Vitek J, Cole T, Speiser PW, New MI, White PC, Pascoe L** 1993 Mutations in the CYP11B1 gene causing congenital adrenal hyperplasia and hypertension cluster in exons 6, 7, and 8. Proc Natl Acad Sci USA 90:4552–4556
12. **Karnak I, Senocak ME, Göğüçş S, Büyükpamukçu N, Hiçsönmez A** 199 Testicular enlargement in patients with 11-hydroxylase deficiency. J Pediatr Surg 32:756–758
13. **Condon J, Ricketts ML, Whorwood CB, Stewart PM** 1997 Ontogeny and sexual dimorphic expression of mouse type 2 11β-hydroxysteroid dehydrogenase. Mol Cell Endocrinol 127:121–128
14. **Paterson JM, Seckl JR, Mullins JJ** 2005 Genetic manipulation of 11β-hydroxysteroid dehydrogenases in mice. Am J Physiol Regul Integr Comp Physiol 289:R642–R652
15. **Draper N, Walker EA, Bujalska IJ, Tomlinson JW, Chalder SM, Arlt W, Lavery GG, Bedendo O, Ray DW, Laing I, Malunowicz E, White PC, Hewison M, Mason PJ, Connell JM, Shackleton CH, Stewart PM** 2003 Mutations in the genes encoding 11β-hydroxysteroid dehydrogenase type 1 and hexose-6-phosphate dehydrogenase interact to cause cortisone reductase deficiency. Nat Genet 34:434–439
16. **Gambineri A, Vicennati V, Genghini S, Tomassoni F, Pagotto U, Pasquali R, Walker BR** 2006 Genetic variation in 11β-hydroxysteroid dehydrogenase type 1 predicts adrenal hyperandrogenism among lean women with polycystic ovary syndrome. J Clin Endocrinol Metab 91:2295–2302
17. **White PC** 2005 Genotypes at 11β-hydroxysteroid dehydrogenase type 1B and hexose-6-phosphate dehydrogenase loci are not risk factors for apparent cortisone reductase deficiency in a large population-based sample. J Clin Endocrinol Metab 90:5880–5883
18. **San Millan JL, Botella-Carretero JI, Alvarez-Blasco F, Luque-Ramirez M, Sancho J, Moghetti P, Escobar-Morreale HF** 2005 A study of the hexose-6-phosphate dehydrogenase gene R453Q and 11β-hydroxysteroid dehydroge

nase type 1 gene 83557insA polymorphisms in the polycystic ovary syndrome. J Clin Endocrinol Metab 90:4157–4162
19. **Kotelevtsev Y, Brown RW, Fleming S, Kenyon C, Edwards, CRW, Seckl JR Mullins JJ** 1999 Hypertension in mice lacking 11β-hydroxysteroid dehydrogenase type 2. J Clin Invest 103:683–689
20. **Jiang JQ, Wang DS, Senthilkumaran B, Kobayashi T, Kobayashi HK, Yamaguchi A, Ge W, Young G, Nagahama Y** 2003 Isolation, characterization and expression of 11β-hydroxysteroid dehydrogenase type 2 cDNAs from the testes of Japanese eel (*Anguilla japonica*) and Nile tilapia (*Oreochromis niloticus*). J Mol Endocrinol 31:305–315
21. **Kusakabe M, Nakamura I, Young G** 2003 11β-Hydroxysteroid dehydrogenase complementary deoxyribonucleic acid in rainbow trout: cloning, sites of expression, and seasonal changes in gonads. Endocrinology 144:2534–2545
22. **Verrijdt G, Schauwaers K, Haelens A, Rombauts W, Claessens F** 2002 Functional interplay between two response elements with distinct binding characteristics dictates androgen specificity of the mouse sex-limited protein enhancer. J Biol Chem 277:35191–35201
23. **Yazawa T, Mizutani T, Yamada K, Kawata H, Sekiguchi T, Yoshino M, Kajitani T, Shou Z, Umezawa A, Miyamoto K** 2006 Differentiation of adult stem cells derived from bone marrow stroma into Leydig or adrenocortical cells. Endocrinology 147:4104–4111
24. **Yazawa T, Mizutani T, Yamada K, Kawata H, Sekiguchi T, Yoshino M, Kajitani T, Shou Z, Miyamoto K** 2003 Involvement of cyclic adenosine 5′-monophosphate response element-binding protein, steroidogenic factor 1, and Dax-1 in the regulation of gonadotropin-inducible ovarian transcription factor 1 gene expression by follicle-stimulating hormone in ovarian granulosa cells. Endocrinology 144:1920–1930
25. **Yazawa T, Nakayama Y, Fujimoto K, Matsuda Y, Abe K, Kitano T, Abe S, Yamamoto T** 2003 Abnormal spermatogenesis at low temperatures in the Japanese red-bellied newt, *Cynops pyrrhogaster*: possible biological significance of the cessation of spermatocytogenesis. Mol Reprod Dev 66:60–66
26. **Miura T, Yamauchi K, Nagahama Y, Takahashi H** 1991 Induction of spermatogenesis in male Japanese eel, *Anguilla japonica*, by a single injection of human chorionic gonadotropin. Zool Sci 8:63–73
27. **Shiina H, Matsumoto T, Sato T, Igarashi K, Miyamoto J, Takemasa S, Sakari M, Takada I, Nakamura T, Metzger D, Chambon P, Kanno J, Yoshikawa H, Kato S** 2006 Premature ovarian failure in androgen receptor-deficient mice. Proc Natl Acad Sci USA 103:224–229
28. **Val P, Jeays-Ward K, Swain A** 2006 Identification of a novel population of adrenal-like cells in the mammalian testis. Dev Biol 299:250–256
29. **O'Shaughnessy PJ, Fleming LM, Jackson G, Hochgeschwender U, Reed P, Baker PJ** 2003 Adrenocorticotropic hormone directly stimulates testosterone production by the fetal and neonatal mouse testis. Endocrinology 144:3279–3284
30. **Wang XL, Bassett M, Zhang Y, Yin S, Clyne C, White PC, Rainey WE** 2000 Transcriptional regulation of human 11β-hydroxylase (hCYP11B1). Endocrinology 141:3587–3594
31. **Takayama K, Morohashi K, Honda S, Hara N, Omura T** 1994 Contribution of Ad4BP, a steroidogenic cell-specific transcription factor, to regulation of the human CYP11A and bovine CYP11B genes through their distal promoters. J Biochem (Tokyo) 116:193–203
32. **Rainey WE** 1999 Adrenal zonation: clues from 11β-hydroxylase and aldosterone synthase. Mol Cell Endocrinol 151:151–160
33. **Gondo S, Yanase T, Okabe T, Tanaka T, Morinaga H, Nomura M, Goto K, Nawata H** 2004 SF-1/Ad4BP transforms primary long-term cultured bone marrow cells into ACTH-responsive steroidogenic cells. Genes Cells 9:1239–1247
34. **Ikeda Y, Lala DS, Luo X, Kim E, Moisan MP, Parker KL** 1993 Characterization of the mouse FTZ-F1 gene, which encodes a key regulator of steroid hydroxylase gene expression. Mol Endocrinol 7:852–860
35. **Morohashi K** 1999 Gonadal and extragonadal functions of Ad4BP/SF-1: developmental aspects. Trends Endocrinol Metab 10:169–173
36. **Parker KL, Schimmer BP** 1997 Steroidogenic factor 1: a key determinant of endocrine development and function. Endocr Rev 18:361–377
37. **Morohashi K, Iida H, Nomura M, Hatano O, Honda S, Tsukiyama T, Niwa O, Hara T, Takakusu A, Shibata Y, Omura T** 1994 Functional difference between Ad4BP and ELP, and their distributions in steroidogenic tissues. Mol Endocrinol 8:643–653
38. **Morohashi K** 1997 The ontogenesis of the steroidogenic tissues. Genes Cells 2:95–106
39. **Borg B** 1994 Androgens in teleost fishes. Comp Biochem Physiol 109:219–245
40. **Lokman PM, Harris B, Kusakabe M, Kime DE, Schulz RW, Adachi S, Young G** 2002 11-Oxygenated androgens in female teleosts: prevalence, abundance, and life history implications. Gen Comp Endocrinol 129:1–12
41. **Liu S, Govoroun M, D'Cotta H, Ricordel MJ, Lareyre JJ, McMeel OM, Smith T, Nagahama Y, Guiguen Y** 2000 Expression of cytochrome P450(11β) (11β-hydroxylase) gene during gonadal sex differentiation and spermatogenesis in rainbow trout, *Oncorhynchus mykiss*. J Steroid Biochem Mol Biol 75:291–298
42. **Yokota H, Abe T, Nakai M, Murakami H, Eto C, Yakabe Y** 2005 Effects of 4-tert-pentylphenol on the gene expression of P450 11β-hydroxylase in the gonad of medaka (*Oryzias latipes*). Aquat Toxicol 71:121–132
43. **Socorro S, Martins RS, Deloffre L, Mylonas CC, Canario AV** 2007 A cDNA for European sea bass (*Dicentrachus labrax*) 11β-hydroxylase: gene expression during the thermosensitive period and gonadogenesis. Gen Comp Endocrinol 150:164–173
44. **Hsueh AJ, Erickson GF** 1978 Glucocorticoid inhibition of FSH-induced estrogen production in cultured rat granulosa cells. Steroids 32:639–648
45. **Valli G, Sudha S, Ravi Sankar B, Govindarajulu P, Srinivasan N** 2000 Altered corticosterone status impairs steroidogenesis in the granulosa and thecal cells of Wistar rats. J Steroid Biochem Mol Biol 73:153–158
46. **Fru KN, VandeVoort CA, Chaffin CL** 2006 Mineralocorticoid synthesis during the periovulatory interval in macaques. Biol Reprod 75:568–574
47. **Hu YC, Wang PH, Yeh S, Wang RS, Xie C, Xu Q, Zhou X, Chao HT, Tsai MY, Chang C** 2004 Subfertility and defective folliculogenesis in female mice lacking androgen receptor. Proc Natl Acad Sci USA 101:11209–11214
48. **Matsubara H LP, Senaha A, Kazeto Y, Ijiri S, Kambegawa A, Hirai T, Youg G, Todo T, Adachi S, Yamauchi K** 2003 Synthesis and possible function of 11-ketotestosterone during oogenesis in eel (*Anguilla japonica*). Fish Physiol Biochem 28:353–354

Endocrinology is published monthly by The Endocrine Society (http://www.endo-society.org), the foremost professional society serving the endocrine community.

In Vitro Cell.Dev.Biol.—Animal (2007) 43:129–138
DOI 10.1007/s11626-007-9021-9

Chromosomal instability in human mesenchymal stem cells immortalized with human papilloma virus E6, E7, and hTERT genes

Masao Takeuchi · Kikuko Takeuchi · Arihiro Kohara · Motonobu Satoh · Setsuko Shioda · Yutaka Ozawa · Azusa Ohtani · Keiko Morita · Takashi Hirano · Masanori Terai · Akihiro Umezawa · Hiroshi Mizusawa

Received: 25 January 2007 / Accepted: 27 March 2007 / Published online: 21 May 2007 / Editor: J. Denry Sato

Abstract Human mesenchymal stem cells (hMSCs) are expected to be an enormous potential source for future cell therapy, because of their self-renewing divisions and also because of their multiple-lineage differentiation. The finite lifespan of these cells, however, is a hurdle for clinical application. Recently, several hMSC lines have been established by immortalized human telomerase reverse transcriptase gene (hTERT) alone or with hTERT in combination with human papillomavirus type 16 E6/E7 genes (E6/E7) and human proto-oncogene, Bmi-1, but have not so much been characterized their karyotypic stability in detail during extended lifespan under in vitro conditions. In this report, the cells immortalized with the hTERT gene alone exhibited little change in karyotype, whereas the cells immortalized with E6/E7 plus hTERT genes or Bmi-1, E6 plus hTERT genes were unstable regarding chromosome numbers, which altered markedly during prolonged culture. Interestingly, one unique chromosomal alteration was the preferential loss of chromosome 13 in three cell lines, observed by fluorescence in situ hybridization (FISH) and comparative-genomic hybridization (CGH) analysis. The four cell lines all maintained the ability to differentiate into both osteogenic and adipogenic lineages, and two cell lines underwent neuroblastic differentiation. Thus, our results were able to provide a step forward toward fulfilling the need for a sufficient number of cells for new therapeutic

M. Takeuchi (✉) · K. Takeuchi · A. Kohara · S. Shioda · Y. Ozawa · A. Ohtani · H. Mizusawa
Division of Bioresources,
National Institute of Biomedical Innovation,
Osaka 567-0085, Japan
e-mail: takeuchim@nibio.go.jp

K. Takeuchi
e-mail: takeuchik@nibio.go.jp

A. Kohara
e-mail: kohara@nibio.go.jp

S. Shioda
e-mail: shioda@nibio.go.jp

Y. Ozawa
e-mail: ozaway@nibio.go.jp

A. Ohtani
e-mail: aohtani@nibio.go.jp

H. Mizusawa
e-mail: mizusawa@nibio.go.jp

M. Satoh
Health Science Research Resources Bank,
Osaka 590-0535, Japan
e-mail: satoh@osa.jhsf.or.jp

K. Morita · T. Hirano · A. Umezawa
National Research Institute for Child Health and Development,
Tokyo 157-8535, Japan

K. Morita
e-mail: morita-keiko@aist.go.jp

T. Hirano
e-mail: hirano-takashi@aist.go.jp

A. Umezawa
e-mail: umezawa@1985.jukuin.keio.ac.jp

M. Terai
Department of Reproductive Biology
and Pathology and Innovative Surgery,
National Research Institute for Child Health and Development,
Tokyo 157-8535, Japan
e-mail: terai@nch.go.jp

applications, and substantiate that these cell lines are a useful model for understanding the mechanisms of chromosomal instability and differentiation of hMSCs.

Keywords Human cord blood mesenchymal stem cell · Long-term culture · Karyotype analysis · mFISH CGH · Differentiation

Introduction

Tissue-specific stem cells in various adult tissues are known to be an important source in the regeneration of damaged tissue and maintenance of homeostasis in the tissues in which they reside. Among these stem cells, human mesenchymal stem cell (hMSC) has recently become of great interest in regenerative medicine, not only to replenish their own tissues, but also to give rise to more committed progenitor cells, which can differentiate into other tissues. MSCs in bone marrow have been shown to differentiate into several types of cell such as osteoblasts, adipocytes, chondrocytes, myocytes, and probably also neuronal cells (Okamoto et al. 2002; Takeda et al. 2004; Mori et al. 2005; Saito et al. 2005; Terai et al. 2005). Because of these properties, it is expected that hMSCs are an enormous potential source for future cell therapy. The goal of our study is to establish cell lines with long lifespan and with parental properties for clinical application. However, clinical application using these cells has been met with enormous difficulty, e.g., isolation of a cell population with specific criteria, expansion in vitro system for obtaining a sufficient number of cells without affecting their genomic characteristics and differentiation properties, and their storage in higher viability.

At present, there is a little evidence suggesting whether changes in these properties occur during expansion. Human normal MSCs have a limited capacity to replicate in the 40- to 50-population doubling level (PDL) at the most. To extend their lifespan, we have previously established human mesenchymal cell lines from human umbilical cord blood or bone marrow by immortalization with human telomerase reverse transcriptase (hTERT), human papillomavirus high-risk type 16 E6/E7 genes (HPV16E6/E7) or polycomb gene, Bmi-1 (Takeda et al. 2004; Mori et al. 2005; Terai et al. 2005).

hTERT-immortalization without affecting biological characteristics, despite extensive proliferation, has been reported in bone-marrow-derived hMSCs (Burns et al. 2005), human fibroblast (Milyavsky et al. 2003), and human keratinocyte (Harada et al. 2003), although it has been indicated that there is the possibility that prolonged culture of hTERT-immortalized fibroblasts may favor the appearance of clones carrying potentially malignant alterations (Milyavsky et al. 2003). HPV16, which encodes oncogenes (E6 and E7), can also immortalize hMSCs in vitro. Both E6 and E7 proteins act through their association with tumor suppressor gene products, p53 and retinoblastoma family members (pRb), respectively. E6 accelerates the degradation of the p53 protein, which is essential for cell arrest at the checkpoint in G_1/S and at the mitotic checkpoint when tetraploidy occurs (Cross et al. 1995), as well as at the G_2 phase under damaging conditions. E7 protein binds to pRb and abrogates the repressive function of these cell cycle regulations (Zheng et al. 2001). Thus, both p53 and pRb play a multitude of important roles in cell-cycle-progression checkpoints as reported in human keratinocytes (Patel et al. 2004), and fibroblasts (Khan et al. 1998). As a consequence, the disruption of the checkpoints that govern accurate cell division leads to abnormal segregation of chromosome and genomic instability, as shown in the cells immortalized with HPV16E6/E7 genes (Duensing et al. 2002).

In this paper, we report on the chromosomal instability and the differentiation activity during prolonged culture (cell expansion) using four mesenchymal stem cell lines. These results indicate that an umbilical cord blood-derived clone immortalized with hTERT (UCBTERT-21) showed normal karyotype for a period of 1 yr, whereas three other cell lines immortalized with HPV16E6/E7 and hTERT or HPV16E6, Bmi-1 and hTERT showed chromosomal instability but maintained the ability to differentiate.

Materials and Methods

Cell culture. Human mesenchymal stem cell lines, UCB TERT-21 (JCRB1107), UCB408E6E7TERT-33 (JCRB1110), UE6E7T-3 (JCRB1136), and UBE6T-6 (JCRB1140) were obtained from the JCRB Cell Bank (Osaka, Japan). Two of them are cell lines obtained by immortalizing human umbilical cord blood mesenchymal stem cells (UCB) with hTERT alone (UCBTERT-21; Terai et al. 2005) or with HPV16E6/E7 in combination with hTERT (UCB408E6E7TERT-33; Terai et al. 2005), and the two others are human bone-marrow-derived mesenchymal stem cell lines transformed with HPV16E6/E7 and hTERT genes (UE6E7T-3; Mori et al. 2005) or with bmi-1, HPV16E6 and hTERT genes (UBE6T-6; Takeda et al. 2004; Mori et al. 2005).

The UCBTERT-21 and UCB408E6E7TERT-33 were grown in PLUSOID-M medium (Med-Shirotori Co., Tokyo, Japan) or MSCGM BulletKit (Cambrex Co., East Rutherford, NJ). UE6E7T-3 and UBE6T-6 were cultured in POWEREDBY10 medium (Med-Shirotori Co.) or MSCGM BulletKit (Cambrex Co.); 5×10^3 cells/ml of each cell line were seeded and cultured for 7–10 d. When culture

plate was subconfluent, cells were treated with 0.25% trypsin/0.5 mM EDTA solution (both from Invitrogen, Tokyo, Japan) and replated at a density of 5×10^3 cells/ml.

All of the cells were maintained in a humidified incubator at 37° C and 5% CO_2. PDLs were calculated using the formula: PDL= log (cell output/input)/log2. At the starting cultivation, PDLs of UCBTERT-21, UCB408E6E7 TERT-33, UE6E7T-3, and UBE6T-6 were 42, 67, 60, and 56, respectively. The doubling time of the UCB408E6E7T-33 cell was 1.5 d, and that of UCBTERT-21, UE6E7T-3, or UBE6T-6 was 2.6, 2.0, or 4.0 days, respectively.

Measurement of chromosome number and fluorescence in situ hybridization. Metaphase chromosome spreads for measurement of chromosome number and fluorescence in situ hybridization (FISH) were prepared from exponential growing cells at various PDL. The cells were treated in a hypotonic solution after exposure to 0.06 μg/ml colcemid (Invitrogen, Carlsbad, CA) for 2 h and fixed in methanol/acetic acid (3:1). The cells were spread on a microscope slide.

To count the number of chromosomes, the cells were stained with DAPI (4′-6-diaminido-2-phenylindol; Vector Laboratories, Inc. Burlingame, CA) and examined under an Axioplan II imaging microscope (Carl Zeiss, GmbH) equipped with Leica QFISH software (Leica Microsystems Holding, UK). To examine statistically significant chromosome numbers, we have allowed ±1 deviation and 50–100 metaphase spreads were scored for each assay.

Painting probes specific for chromosome 13 (XCP13-kit, FITC; MetaSystems, GmbH) and chromosome 17 (XCP17-kit; Texas Red) (MetaSystems GmbH, Altlussheim, Germany), and multicolor probes (mFISH-24Xcyte-kit, DAPI, FITC, TexasRed, Cy3, Cy5, and DEAC; MetaSystems GmbH) were used for FISH analysis. FISH was performed according to the manufacture's protocol (MetaSystems GmbH). Briefly, both the metaphase chromosome spread and the probe were denatured with 0.07 N NaOH or 70% formamide, hybridized at 37° C for 1–4 d, and counterstained with DAPI. FISH images were captured and analyzed on the Zeiss Axio Imaging microscope (Carl Zeiss Microimaging GmbH, Jena, Germany) with Isis mBAND/mFISH imaging Software (MetaSystems GmbH).

CGH analysis. Hybridization was carried out with the BAC Array (MAC ArrayTM Karyo 4000 Component, Macrogen Co., Rockville, MD) by the Hybstation (Genomic Solutions, Ann Arbor, MI). Briefly, test DNAs, which were isolated using an isolation kit (Amersham BioSciences, Little Chalfont, UK) and Spin Column (QIAGEN Co., Tokyo, Japan), and reference DNAs (Promega Co., Madison, WI), were labeled, respectively, with Cy3 or Cy5 (BioPrimer DNA Labeling System, Invitrogen Co.), precipitated together with ethanol in the presence of Cot-1 DNA, redissolved in a hybridization mixture (50% formamide, 10% dextran sulfate, 2xSSC, 4% sodium dodecyl sulfate [SDS], pH 7), and denatured at 75° C for 10 min. After incubation at 37° C for 30 min, each mixture was applied to an array slide and incubated at 42° C for 48–72 h. After hybridization, the slides were washed in a solution of 50% formamide—2× SSC (pH 7.0) for 15 min at 50° C, in 2× SSC—0.1% SDS for 15 min at 50° C, and in a 100-mM sodium phosphate buffer containing 0.1% Nonidet P-40 (pH 8) for 15 min at room temperature, then scanned with GenePix4000A (Axon Instruments, Union City, CA). Acquired images were analyzed with MacViewer (Macrogen Instruments).

Differentiation ability. To evaluate the differentiation potential of each cell line, cells were cultured on a coverslip in each induction medium, that is, hMSC Differentiation BulletKit-Adipogenic (PT-3004, Cambrex BioScience, Inc., Walkersville, MD) for adipocyte and NPMM Bullet kit (NPMM™ BulletKit (B3209, Cambrex BioScience) for neural progenitor cells. For osteoblast, cells were treated with 0.1 μM dexamethasone (Sigma Chemical Co., St. Louis, MO), 50 μg/ml L-ascorbic acid (Sigma Chemical), and 10 mM β-glycerophosphate (Sigma Chemical) in the PLUSOID-M medium (Med-Shirotori Co.) or the POWER-EDBY10 medium (Med-Shirotori Co.) of culture medium.

After 2–4 wk, the cells were washed in phosphate-buffered saline (PBS), fixed in 4% paraformaldehyde in PBS and stained with Oil Red-O (Sigma Chemical) for detection of adipocyte, and with alkaline phosphatase staining solution containing 0.25 mg/ml naphthol AS-BI phosphate and 0.25 mg/ml Fast violet LB salt for detection of alkaline phosphatase-positive osteoblast. In immunostaining for neuron-like cells, the cells fixed with paraformaldehyde were permeabilized with methanol at −20° C for 10 min and stained with an anti-IIIβ tubulin antibody (Sigma Chemical) or anti-neurofilament antibody NF-200 (Sigma Chemical) and Texas Red-anti-mouse IgG (Southern Biotechnology Associates, Inc., Birmingham, AL) as previously described (Takeuchi et al. 1990).

Results

Changes in chromosomal number in human mesenchymal stem cell lines in prolonged culture. Immortalization of cultured cells frequently induces an abnormal chromosome number as shown in cancer cells (Duensing et al. 2000; Munger et al. 2004; Patel et al. 2004), especially at higher frequency in long-term culture. We therefore examined four cell lines, human mesenchymal stem cell (hMSC) lines immortalized with combinations of bmi-1, E6, E7, and/or hTERT genes, for chromosome instability by counting metaphase chromosomes.

All of the lines were diploid, each containing 46 up to 40 PDL including the PDL numbers of nontransfecting original MSCs (Takeda et al. 2004; Mori et al. 2005; Terai et al. 2005). For UCBTERT-21 cell, no further changes in chromosome number have been observed up to date (for PDL 133) as shown in Fig. 1*A* and *B*. In contrast, although the UBE6T-6 cell and the UE6E7T-3 cell were near diploid, both cells exhibited considerable variation in chromosome number from PDL 70 after the culture started. For example, when the assay of UE6E7T-3 cells start at PDL 62 in culture, 90% of cell population had 46 chromosomes, but the population decreased with prolonged culturing and a population containing 44 chromosomes became dominant (43% of cell populations) at PDL 147 (Fig. 1*E*, *F*). A similar variation was also observed in UBE6T-6 cells (Fig. 1*C*, *D*).

To ascertain whether or not the changes observed were induced by transfection with HPV16E6E7, we assayed the chromosome numbers of UCB408E6E7TERT-33 cell in prolonged culture. The cell line showed similar chromosomal changes to those of the UE6E7T-3 cell, the rate of which was more rapid. At day 2 after culture by us changes became evident (PDL 68), the UCB408E6E7TERT-33 cells consisted of two distinct populations concerning chromosome number (near diploid [24%] and near tetraploid [53%]), shown in Fig. 1*G*. However, the near diploid population was unstable and decreased gradually. At PDL 81, the population became only near tetraploid, 80% of the

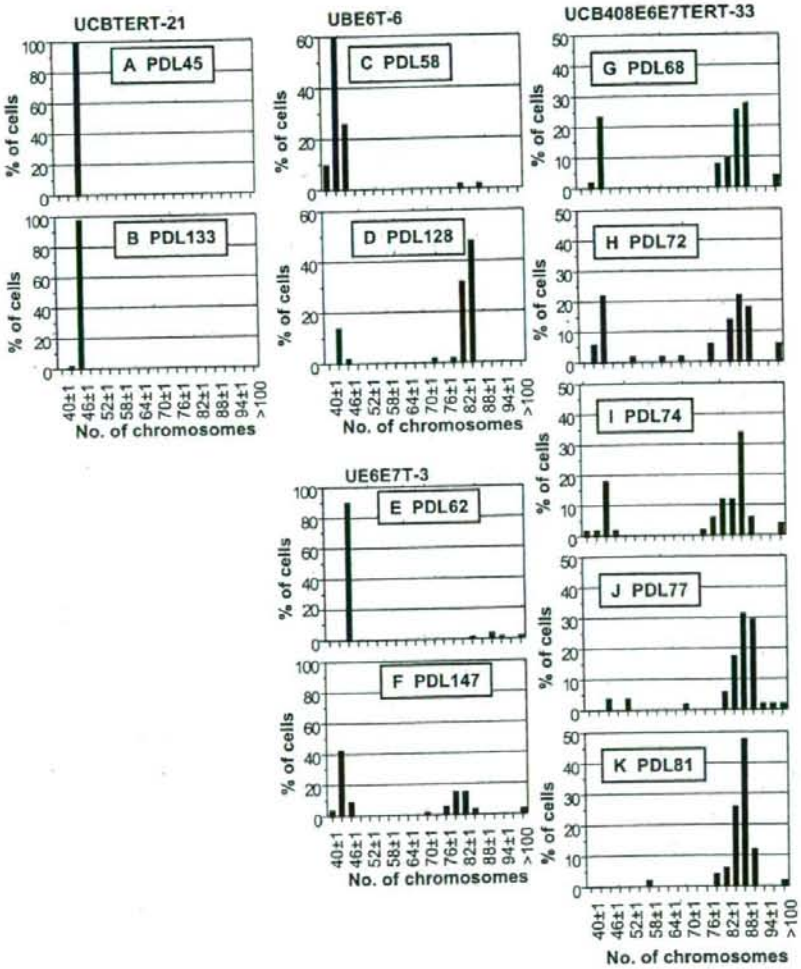

Figure 1. Changes in chromosomal numbers in prolonged cultures of four hMSC cell lines. (*A–K*) The chromosomal numbers at various culture stages were counted by DAPI staining. (*A*, *B*), (*C*, *D*), (*E*, *F*), and (*G–K*) represent the chromosomal numbers from UCBTERT-21, UBE6T-6, UE6E7T-3, and UCB408E6E7TERT-33, respectively. To examine statistically significant chromosomal numbers, we have allowed ±1 deviation, and 50–100 metaphase spreads were examined for each assay. *Note* the changes in chromosomal number from near 2*n* to near 4*n* in prolonged culture.